Two transmembrane transcriptional regulators coordinate to activate chitin-induced natural transformation in *Vibrio cholerae*

Allison C. Hullinger[1,†], Virginia E. Green[1,†], Catherine A. Klancher[1], Triana N. Dalia[1], and Ankur B. Dalia[1,*]

[1]Department of Biology, Indiana University, Bloomington, IN 47405.
[†]These authors contributed equally to this work.
*Corresponding author: ankdalia@iu.edu

ABSTRACT

Transcriptional regulators are a broad class of proteins that alter gene expression in response to environmental stimuli. Transmembrane transcriptional regulators (TTRs) are a subset of transcriptional regulators in bacteria that can directly regulate gene expression while remaining anchored in the membrane. Whether this constraint impacts the ability of TTRs to bind their DNA targets remains unclear. *Vibrio cholerae* uses two TTRs, ChiS and TfoS, to activate horizontal gene transfer by natural transformation in response to chitin by inducing the *tfoR* promoter (P_{tfoR}). While TfoS was previously shown to bind and regulate P_{tfoR} directly, the role of ChiS in P_{tfoR} activation remains unclear. Here, we show that ChiS directly binds P_{tfoR} upstream of TfoS, and that ChiS directly interacts with TfoS. By independently disrupting ChiS-P_{tfoR} and ChiS-TfoS interactions, we show that ChiS-P_{tfoR} interactions play the dominant role in P_{tfoR} activation. Correspondingly, we show that in the absence of ChiS, recruitment of the P_{tfoR} locus to the membrane is sufficient for P_{tfoR} activation when TfoS is expressed at native levels. Finally, we show that the overexpression of TfoS can bypass the need for ChiS for P_{tfoR} activation. All together, these data suggest a model whereby ChiS both (1) recruits the P_{tfoR} DNA locus to the membrane for TfoS and (2) directly interacts with TfoS to increase its local concentration near the membrane-proximal promoter. This work furthers our understanding of the molecular mechanisms that drive chitin-induced responses in *V. cholerae* and more broadly highlights how the membrane-embedded localization of TTRs can impact their activity.

INTRODUCTION

Bacterial species inhabit diverse environments where they encounter a wide range of stressors. To survive fluctuating conditions, they must have ways to sense and respond to environmental change. One such mechanism is the alteration of gene expression in response to specific environmental cues using a broad group of proteins called transcriptional regulators. Most commonly, transcriptional regulators are localized to the cytoplasm, where they can freely diffuse to find their DNA targets. However, recent work highlights the presence of transmembrane transcriptional regulators (TTRs) in diverse bacterial genomes [1]. In the few examples where they have been studied, TTRs were shown to bind to their DNA targets while remaining anchored in the membrane [2-7]. However, TTRs remain relatively poorly characterized, and the factors that influence how TTRs find their DNA targets to regulate gene expression remain unclear. Here, we investigate the mechanism of action for two chitin-responsive TTRs in *Vibrio cholerae*—TfoS and ChiS.

TfoS is a TTR that is required for induction of horizontal gene transfer by natural transformation. Previous work shows that TfoS directly activates the expression of the small RNA (sRNA) *tfoR*

by binding to its promoter (P_{tfoR}) [8, 9]. When transcribed, *tfoR* base pairs with the 5' untranslated region (UTR) of the mRNA of the master regulator of competence, TfoX, which allows for its translation [10]. TfoX then activates the expression of the genes necessary for DNA uptake and integration [11, 12].

ChiS is a TTR that is critical for induction of the chitin utilization program in *V. cholerae* [13, 14]. Specifically, ChiS binds to the promoter of the chitobiose (*chb*) utilization operon (P_{chb}) to activate the expression of genes required for chitin uptake and catabolism [4, 14]. Like TfoS, ChiS is critical for chitin-induced natural transformation [8, 9]. However, it is unclear whether this is due to its role in promoting chitin catabolism or a more direct impact of ChiS on regulating the genes required for natural transformation. Previous studies demonstrate that ChiS and TfoS are both required for chitin-induced P_{tfoR} activation, supporting the latter possibility [8, 9]. However, the mechanism by which ChiS and TfoS coordinate to regulate P_{tfoR} expression remains unclear.

RESULTS

ChiS binds to P_{tfoR} and is required for P_{tfoR} activation

Prior work suggests that ChiS and TfoS are both required for activation of P_{tfoR} [8, 9]. To formally test this, we generated strains with a chromosomally integrated P_{tfoR}-*gfp* transcriptional reporter. These strains also contained a previously described P_{chb}-*mCherry* construct [15], which serves as a reporter for ChiS activity. In addition, these strains contained a constitutively expressed [16] mTFP1 construct (P_{const2}-*mTFP1*), which was used to normalize for intrinsic noise in gene expression. When a strain harboring these constructs was incubated on chitin, we observed strong activation of both P_{tfoR} and P_{chb} by fluorescence microscopy, consistent with their known regulation by chitin [4, 10]. Deleting either *chiS* or *tfoS* resulted in a complete loss of P_{tfoR} activation (**Fig. 1 A-B**). Furthermore, we found that P_{chb} expression was completely ablated by Δ*chiS*, but not by Δ*tfoS* (**Fig. 1C**), which is consistent with the previously established role for ChiS in P_{chb} activation [4, 14]. These results confirm that both ChiS and TfoS are required for P_{tfoR} induction and demonstrate that these TTRs are not equally required for expression of all chitin-regulated promoters in *V. cholerae*.

The downstream consequence of P_{tfoR} induction is the expression of the genes necessary for horizontal gene transfer by natural transformation. We therefore also assessed the phenotypic impact of P_{tfoR} regulation by ChiS and TfoS on natural transformation. We found that mutation of either *chiS* or *tfoS* reduced natural transformation to the limit of detection (**Fig. 1D**), which is consistent with a critical role for both TTRs in inducing this behavior. Further, the overexpression of *tfoR* restores natural transformation in both Δ*chiS* and Δ*tfoS* backgrounds, suggesting that the inability of these strains to transform is due to the lack of *tfoR* expression (**Fig. S1**).
Our previous work has established that TfoS directly binds P_{tfoR} and that the ectopic expression of TfoS in the heterologous host *E. coli* is sufficient to drive P_{tfoR} induction even in the absence of ChiS [9]. However, our results above demonstrate that ChiS is still necessary for P_{tfoR} activation in *V. cholerae*. Thus, one possibility is that ChiS is necessary to stabilize natively expressed TfoS in *V. cholerae* (*i.e.,* that native TfoS is degraded in the absence of ChiS). To test this hypothesis, we generated a functional FLAG-tagged allele of TfoS (**Fig. S2**) and performed Western blot analysis. We found that TfoS expression is not altered in the Δ*chiS* background (**Fig. S2C**). This result suggests that ChiS does not promote P_{tfoR} activation by simply stabilizing TfoS.

Because ChiS does not stabilize TfoS, we reasoned that it may play a more active role in regulating P_{tfoR}. Specifically, we hypothesized that ChiS may directly bind to P_{tfoR}. To test this possibility, we performed chromatin immunoprecipitation-sequencing (ChIP-seq) to identify ChiS

binding sites *in vivo*. Consistent with previous work from our lab demonstrating that ChiS binds to P_{chb} [4], we observed a strong ChIP peak at the P_{chb} promoter (**Fig. 1E**). This analysis also revealed a strong ChIP peak at P_{tfoR} (**Fig. 1E**). To verify this result, we performed electrophoretic mobility shift assays (EMSAs) using the purified cytoplasmic domain of ChiS and found that it binds to P_{tfoR} *in vitro* (**Fig. 1F**). Furthermore, we show that this interaction could be competitively inhibited by unlabeled P_{tfoR} probe but not by a nonspecific promoter probe ($P_{VCA0053}$) (**Fig. 1F**), indicating that the interaction of ChiS with P_{tfoR} is specific. Together, these results indicate that both ChiS and TfoS bind P_{tfoR}, and that both TTRs are critical for chitin-induced expression of TfoR.

ChiS directly interacts with TfoS

Our results thus far are consistent with two possible models for activation of P_{tfoR} by ChiS and TfoS. One possibility is that TfoS cannot bind P_{tfoR} independently, but instead relies on ChiS binding at P_{tfoR} to recruit this DNA locus to the membrane so that it becomes accessible to TfoS. Alternatively, ChiS may bind alongside TfoS at P_{tfoR} and then directly interact with TfoS to allosterically regulate its activity by inducing a conformational change that allows TfoS to bind P_{tfoR}. One of the primary differences between these two models is that the latter has a strict requirement for a direct interaction between ChiS and TfoS, while the former model does not. To test whether ChiS and TfoS interact, we performed PopZ linked apical recruitment (POLAR) assays [17]. In these assays, two putatively interacting proteins, the “bait” and the “prey”, are translationally fused to distinct fluorescent markers to track their independent localization. The bait protein is also fused to an H3H4 PopZ interaction domain derived from *Caulobacter crescentus*. Upon induction of the polarly localizing PopZ protein, the bait is relocalized to the cell pole. If the prey interacts with the bait, it will also relocalize to the cell pole. If there is no interaction between the bait and prey, the localization of the prey should be unaffected by PopZ induction. To assess interactions between ChiS and TfoS, we generated strains expressing ChiS-msfGFP-H3H4, TfoS-mCherry, and arabinose-inducible PopZ. In the absence of ChiS, TfoS was diffusely localized at the cell periphery, consistent with it being a membrane-embedded regulator, and this localization did not change when PopZ was induced (**Fig. 2**). We have previously found that ChiS inherently forms foci at the cell periphery for reasons that remain unclear [4], and we have recapitulated this observation here (**Fig. 2**). We found that in cells expressing both ChiS and TfoS, TfoS forms foci that strongly colocalize with ChiS, suggesting that these proteins may interact (**Fig. 2**). Furthermore, when PopZ is induced in these cells, both ChiS and TfoS relocalize to the cell poles, which is consistent with ChiS-TfoS interactions (**Fig. 2**). As an independent way to assess ChiS-TfoS interactions, we also performed bacterial adenylate cyclase two-hybrid (BACTH) assays. These assays also showed an interaction between ChiS and TfoS, further suggesting that these proteins directly interact (**Fig. S3**).

ChiS-TfoS interactions support, but are not critical for P_{tfoR} activation

We next wanted to test whether the interaction between ChiS and TfoS is critical for P_{tfoR} activation, so we sought to disrupt the interaction between these proteins. To that end, we created a functional chimera called Chi37, which is composed of the two transmembrane domains and a truncated portion of the periplasmic domain of the chemoreceptor Mlp37 translationally fused to the cytoplasmic domain of ChiS. Chi37 is functional for P_{chb} activation and binds both P_{chb} and P_{tfoR} at wildtype levels *in vivo* according to ChIP-qPCR assays (**Fig. S4**). However, POLAR assays demonstrate that Chi37 cannot relocalize TfoS, indicating that Chi37 cannot interact with TfoS (**Fig. 2**). These data suggest that the interaction interface for ChiS and TfoS is within the periplasmic or transmembrane domains of these TTRs. Because Chi37 retains the ability to bind DNA but lacks the ability to interact with TfoS, we used this allele to test the impact of ChiS-TfoS interactions on P_{tfoR} activation.

If the interaction between ChiS and TfoS is essential for P_{tfoR} activation, we hypothesized that a strain harboring Chi37 will not be able to activate P_{tfoR} expression, and therefore will not allow for chitin-induced natural transformation. However, we found that a Chi37 mutant had an intermediate phenotype – it exhibited decreased P_{tfoR} activation and transformation compared to the parent, but this was still significantly greater than Δ*chiS* (**Fig. 3A-C**). Because strains with Chi37 still retained the ability to activate P_{tfoR} to some degree, it suggests that ChiS-TfoS interactions are not strictly required for allosteric regulation of TfoS activity. This result is also consistent with our prior observation that TfoS can induce P_{tfoR} in *E. coli* even in the absence of ChiS [9]. However, these findings also make it clear that the interaction between ChiS and TfoS is important for optimal P_{tfoR} induction.

Overexpression of TfoS bypasses the need for ChiS to activate P_{tfoR}

Because ChiS-TfoS interactions contribute to optimal P_{tfoR} induction, we hypothesized that this interaction might allow ChiS to increase the local concentration of TfoS in the proximity of the membrane-localized P_{tfoR} DNA locus. Based on this model, we hypothesized that the overexpression of TfoS within the cell should bypass the need for ChiS-TfoS interactions for optimal P_{tfoR} activation. Under these conditions, we predicted that the likelihood of TfoS being physically close to a membrane-proximal P_{tfoR} locus should be greatly increased, thereby resulting in restoration of P_{tfoR} activation in the Chi37 background. To test this hypothesis, we generated an IPTG-inducible TfoS construct (P_{tac}-*tfoS*) and confirmed that this construct resulted in overexpression of TfoS via western blot analysis (**Fig. S2**).

Consistent with the proposed model, we found that overexpressing TfoS in the Chi37 background restored P_{tfoR} activation and natural transformation, suggesting that the ChiS-TfoS interactions were no longer necessary due to the increased abundance of TfoS in the cell (**Fig. 3A-C**). Furthermore, we found that overexpression of TfoS overcomes the need for ChiS completely (*i.e.*, overexpression of TfoS recovers P_{tfoR} induction and transformation in the Δ*chiS* background) (**Fig. 3A-C**). This result may suggest that the ChiS-dependent recruitment of P_{tfoR} to the membrane is only required when TfoS is present at native levels; when TfoS is overexpressed, it obviates the need for ChiS by increasing the likelihood that TfoS will come into contact with the P_{tfoR} DNA locus (which will presumably be membrane-proximal at some frequency due to diffusion of the DNA locus within the cell) independently.

The ChiS binding site in P_{tfoR} is critical for activation when TfoS is expressed at native levels

Based on the model suggested above, we hypothesize that the ChiS binding site within P_{tfoR} should be critical for activation when ChiS and TfoS are present at native levels. Based on the sequence of the ChiS Binding Sites (CBS) in P_{chb} [4], a putative CBS within P_{tfoR} was found at the 5' end of the promoter upstream of the TfoS binding site (**Fig. S5**). Indeed, truncating the 5' end of P_{tfoR} prevents ChiS binding (**Fig. S5**). We refer to this truncated promoter construct as $P_{tfoR}^{\Delta CBS}$. The $P_{tfoR}^{\Delta CBS}$ mutation resulted in minimal P_{tfoR} activation and inhibited chitin-induced natural transformation when ChiS and TfoS were present at native levels (**Fig. 3A-B**). Importantly, this strain still contains a functional copy of ChiS, but ChiS can no longer bind at P_{tfoR}. If the loss of *tfoR* expression in $P_{tfoR}^{\Delta CBS}$ is due to a loss of ChiS-dependent recruitment of P_{tfoR} to the membrane, we would predict that overexpression of TfoS should bypass the impact of the $P_{tfoR}^{\Delta CBS}$ mutation (similar to what was observed in Δ*chiS*). Indeed, we found that overexpression of TfoS recovers $P_{tfoR}^{\Delta CBS}$ induction and natural transformation (**Fig. 3A-C**). This result also demonstrates that the truncation used to generate $P_{tfoR}^{\Delta CBS}$ does not simply diminish the activity of this promoter.

In $P_{tfoR}^{\Delta CBS}$, membrane recruitment is eliminated, allowing us to further isolate and test the impact of ChiS-TfoS interactions. The ChiS in $P_{tfoR}^{\Delta CBS}$ can still bind to TfoS and other DNA loci (*e.g.*, at P_{chb}), meaning that ChiS binding to TfoS should still be maintained in this background. In contrast, Chi37 in $P_{tfoR}^{\Delta CBS}$ cannot interact with TfoS, and is therefore incapable of allosteric activation. We found that there was no increase in $P_{tfoR}^{\Delta CBS}$ activation when cells expressed ChiS vs Chi37 (**Fig. 3A-B**). Consistent with this, neither ChiS or Chi37 in the $P_{tfoR}^{\Delta CBS}$ background is capable of supporting chitin-induced natural transformation (**Fig. 3C**). These data suggest that ChiS binding at P_{tfoR} plays a more important role in activation than its interaction with TfoS.

Recruitment of P_{tfoR} to the membrane is sufficient for TfoS-dependent activation

Together, our results suggest that ChiS binding at P_{tfoR} is more important than ChiS binding to TfoS for activation to occur. These data are consistent with two potential models. First, ChiS binding recruits P_{tfoR} to the membrane to make it accessible to TfoS. Alternatively, ChiS binding within P_{tfoR} may alter promoter architecture, which ultimately exposes the TfoS binding site. The distinction between these two models is that for the latter, there would likely be a requirement for native ChiS-CBS interactions within P_{tfoR} to alter promoter architecture. However, for the former model, we would predict that recruiting $P_{tfoR}^{\Delta CBS}$ to the membrane should be sufficient for activation. To test this hypothesis, we took advantage of the Tet repressor (TetR), which naturally binds its operator sequence, *tetO*, at high affinity. Specifically, we replaced the CBS within P_{tfoR} with *tetO* ($P_{tfoR}^{\Delta CBS::tetO}$) and swapped the native DNA-binding domain (DBD) of ChiS for TetR. When we expressed $ChiS^{\Delta DBD}$-TetR in cells containing $P_{tfoR}^{\Delta CBS::tetO}$, we found that induction and natural transformation were recovered when compared to cells lacking the $ChiS^{\Delta DBD}$-TetR construct (**Fig. 4A-C**). To test this further, we incubated strains with anhydrous tetracycline (ATc) to inhibit the DNA-binding activity of TetR. Under these conditions, both P_{tfoR} induction and natural transformation were ablated. This result is consistent with our hypothesis and suggests that recruitment of $P_{tfoR}^{\Delta CBS::tetO}$ to the membrane via $ChiS^{\Delta DBD}$-TetR binding is necessary for activation to occur (**Fig. 4A-C**). This result also argues against ChiS-dependent remodeling of *tfoR* promoter architecture, as native ChiS-CBS interactions have been entirely replaced by those of TetR and *tetO*. Importantly, overexpression of TfoS was able to rescue $P_{tfoR}^{\Delta CBS::tetO}$ induction even in the absence of ChiS, indicating that this promoter is fully functional (**Fig. 4A-C**).

DISCUSSION

In this study, we uncover how ChiS and TfoS coordinate to promote activation of natural transformation in *V. cholerae*. Specifically, our data are most consistent with a model wherein ChiS performs two functions to facilitate P_{tfoR} activation: (1) it recruits the P_{tfoR} DNA locus to the membrane and (2) it directly interacts with TfoS to increase its local concentration near the membrane-proximal promoter (**Fig. 5**).

The downstream effect of *tfoR* expression is the activation of the genes required for DNA uptake and integration by natural transformation. It is hypothesized that natural transformation is induced by chitin oligosaccharides because *Vibrio* species accumulate and form biofilms on chitinous surfaces in the aquatic environment. Thus, chitin is a niche where diverse *Vibrios* are present, and represents an ideal site for genetic exchange. In support of this model, prior work has uncovered that on chitin *V. cholerae* actively lyses neighboring bacteria to release their DNA as a substrate for natural transformation [18, 19].

Our data suggests that simply overexpressing TfoS is sufficient to bypass the requirement for ChiS for P_{tfoR} activation. ChiS and TfoS are likely independently activated by chitin

oligosaccharides [4, 9]. Why then has ChiS-dependent regulation of P_{tfoR} been maintained in *V. cholerae*? One possibility is that this dual requirement ensures that natural transformation is not induced until cells are experiencing conditions where chitin oligosaccharides are abundant. This would prevent the inappropriate expression of the large repertoire of genes required for natural transformation that might incur a significant fitness cost. However, not all genes within the chitin regulon require the dual activity of ChiS and TfoS. For example, the *chb* operon required for chitin uptake and catabolism is largely dependent on ChiS alone as shown in this and prior work [4, 8]. Because nutrient acquisition is likely a prerequisite for natural transformation, it is tempting to speculate that the "relaxed" requirement for chitin-dependent induction of the *chb* operon is to ensure that chitin uptake and catabolism is prioritized over genetic exchange by natural transformation.

Here, we show that ChiS and TfoS are two TTRs that must cooperatively act to promote P_{tfoR} activation. This cooperation between TTRs may be a common feature for this class of transcriptional regulators. Indeed, *V. cholerae* contains another pair of TTRs, ToxRS and TcpPH, that coordinate to activate the *toxT* promoter [5-7, 20, 21]. There are a number of parallels between ToxRS/TcpPH dependent activation of P_{toxT} and ChiS/TfoS dependent activation of P_{tfoR}. Namely, TcpPH is sufficient to activate P_{toxT} when overexpressed, but requires ToxRS for P_{toxT} induction when expressed at native levels [20]. Furthermore, the membrane-embedded localization of ToxRS is required for this stimulatory activity [7, 21]. The ToxRS binding site in P_{toxT} is also located upstream of the TcpPH binding site [7, 20]. These data are consistent with ToxRS facilitating recruitment of P_{toxT} to the membrane for downstream binding and activation by TcpPH. Recent results, however, suggest that ToxRS interactions with P_{toxT} may alter the structure of the promoter to promote TcpPH-dependent activation [5, 6]. TcpPH and ToxRS are members of a rapidly evolving family of signal transduction proteins in enteric bacteria [22]. Thus, other members of this family may also coordinate to regulate their downstream targets. One recent example is VrtAC, which likely coordinates with VtrB to activate the expression and transertion of the type III secretion system in *V. parahaemolyticus* [3]. Not all TTRs require cooperativity for their activity, however. This is true for ChiS at the *chb* promoter [4, 8], ToxR at the *ompU* promoter [20], and *E. coli* CadC at the *cadBA* operon [2].

The localization and diffusion of TTRs is clearly constrained compared to canonical cytoplasmic TRs. However, whether this constraint impacts how TTRs bind to their target sites is not clear. Our results suggest that natively expressed TfoS cannot activate P_{tfoR} unless ChiS is also present and able to bind P_{tfoR}. However, this requirement for ChiS can be overcome by simply overexpressing TfoS. This finding suggests that when natively expressed, TfoS cannot bind to P_{tfoR}. Thus, the accessibility of the DNA binding targets for membrane-constrained TTRs may represent an additional layer of regulation that is a distinct property for this class of regulators when compared to canonical cytoplasmic transcriptional regulators. The DNA targets that TTRs bind must localize proximally to the membrane at some frequency. However, it is unclear if all regions of the genome are equally likely to diffuse and localize near the membrane in this manner. One possibility is that TTRs have evolved to bind to genomic loci that are more likely to come into contact with the membrane. Future work will focus on systematically assessing whether the constraint of membrane localization limits the genomic loci that TTRs can effectively bind and regulate.

Our data are consistent with a model in which membrane recruitment of P_{tfoR} is necessary for TfoS-dependent activation. This could be because TfoS, when expressed at native levels, lacks the ability to bind and recruit P_{tfoR} to the membrane by itself. However, the P_{tfoR} locus is not inherently difficult for a TTR to bind because we show that ChiS naturally binds to this locus from the membrane. Therefore, the P_{tfoR} DNA locus must come into contact with the membrane

305 at some frequency. If so, one interpretation of our data is that TfoS is less capable of stably
306 binding P_{tfoR} at the membrane compared to ChiS. Indeed, kinetic studies of the TTR CadC
307 suggest that the mobility of CadC within the membrane impacts its target search more than the
308 mobility of the DNA itself, which may also suggest that some regions of the genome contact the
309 membrane with such frequency that they do not limit target search [23].
310
311 DNA-binding transcriptional regulators spend a large portion of their time transiently binding to
312 DNA nonspecifically during their target search [24]. This transient binding can keep these
313 proteins in close proximity to the nucleoid and help reduce the dimensionality of the 3D target
314 search for a freely diffusing cytoplasmic DNA-binding protein. Therefore, a distinct possibility is
315 that the membrane localization of TfoS does not make it more difficult for this regulator to bind to
316 DNA. Instead, it could be that TfoS is capable of binding DNA, but does so with a relaxed
317 specificity, which reduces the likelihood that it will identify and bind its sequence-specific target
318 sites within the genome compared to other TTRs like ChiS. If so, ChiS binding at P_{tfoR} may
319 simply "trap" this DNA locus at the membrane and help reduce the dimensionality of the target
320 search for TfoS from a three-dimensional search into a two-dimensional search (due to the
321 constrained diffusion of TfoS within a planar membrane). It is tempting to speculate that other
322 molecular interactions, whether protein-protein or DNA-protein, also take advantage of the
323 membrane as a planar space to increase the specificity and/or efficiency of the target search.
324
325
326 **METHODS**
327 **Bacterial strains and culture conditions**
328 All mutant strains were derived from the *Vibrio cholerae* El Tor strain E7946 [25]. Unless
329 otherwise indicated, *V. cholerae* strains were grown in LB medium or on LB agar. When
330 necessary, LB was supplemented with chloramphenicol (1 µg/mL), kanamycin (50 µg/mL),
331 trimethoprim (10 µg/mL), spectinomycin (200 µg/mL), carbenicillin (100 µg/mL), erythromycin
332 (10 µg/mL), zeocin (100 µg/mL), or sulfamethoxazole (100 µg/mL). A list of all strains used in
333 this study can be found in **Table S1**.
334
335 **Strain construction**
336 Mutant constructs were made using splicing-by-overlap extension (SOE) PCR, as previously
337 described [26]. Chromosomally integrated ectopic expression constructs were used throughout
338 this study as previously described [27]. A list of all primers used to make mutant constructs can
339 be found in **Table S2**. Mutant strains were generated by introducing constructs into strains by
340 natural transformation; either chitin-induced natural transformation or chitin-independent natural
341 transformation via the use of an IPTG-inducible *tfoX* plasmid (pMMB-*tfoX*) *[28].* The pMMB-*tfoX*
342 plasmid was cured before strains were used in any experiments. Mutants were confirmed by
343 PCR and/or sequencing.
344
345 **Chitin-induced natural transformation assays**
346 Strains were grown overnight in LB broth at 30°C rolling. Overnight cultures were then
347 subcultured in LB broth, with 1 µM IPTG when applicable, and grown to mid-log phase (OD_{600}
348 ~0.5-1.0). Cells were washed and resuspended in 0.5X Instant Ocean (IO; 7g/L, Aquarium
349 Systems Inc.). Then, 1 mL chitin reactions were made by mixing 10^8 cells (suspending in 100 µL
350 IO), 150 µL of chitin slurry (8g/150mL, Alfa Aesar), 750 µL IO, and 1 µM IPTG when applicable.
351 Chitin reactions were incubated at 30°C static for ~18 hours. Next, 550 µL of supernatant was
352 removed, and 500 ng of transforming DNA (tDNA) was mixed with the cells by inversion. The
353 tDNA used replaced the frame-shifted transposase gene VC1807 (*i.e.*, a "neutral" gene locus)
354 with either an Erm^R or Cm^R marker. A no tDNA control was included for each strain tested. Cells
355 were incubated with DNA for 5 hours at 30°C static. Then, 500 µL LB broth was added to each

356 reaction, and reactions were outgrown by shaking at 37°C for 2 hours. After outgrowth,
357 reactions were plated for quantitative culture for total viable count (plated on plain LB agar) and
358 transformants (plated on LB agar with antibiotic). Transformation frequency was calculated by
359 dividing the CFU/mL of transformants by the CFU/mL of total viable counts.
360
361 **PopZ-linked apical recruitment (POLAR) assays**
362 Strains were grown overnight in LB broth at 30°C rolling and were supplemented with 10 μM
363 IPTG to induce P_{tac}-*tfoS-mCherry,* P_{tac}-*chiS-GFP-H3H4, and/or* P_{tac}-*chi37-GFP-H3H4*
364 constructs. For POLAR experiments, LB broth was also supplemented with 0.05% arabinose to
365 induce P_{bad}-*PopZ* expression. For efficient polar relocalization and to avoid issues with cell
366 curvature, the curvature determinant *crvA* [29] was deleted in all colocalization strains.
367 Overnight cultures were washed and resuspended in 0.5X IO. Cells were then placed on a glass
368 coverslip beneath a 0.4% IO gelzan pad and imaged using FITC and mCherry filter cubes. Heat
369 maps were generated by analyzing the fluorescence localization of 300 cells per replicate.
370
371 **Microscopy**
372 Cells were imaged on an inverted Nikon Ti-2 microscope with a Plan Apo 60x objective lens, the
373 appropriate filter cubes (FITC, YFP, mCherry, and/or CFP), a Hamamatsu ORCAFlash 4.0
374 camera, and Nikon NIS Elements imaging software. Image analysis was conducted using the
375 MicrobeJ plugin [30] in Fiji [31].
376
377 **Bacterial adenylate cyclase two-hybrid assays**
378 ChiS and TfoS genes were amplified using PCR and cloned into the BACTH vectors pKT25,
379 pUT18C, pKNT25, and pUT18 to generate N- and C-terminal fusions to the T18 and T25
380 fragments of adenylate cyclase. Miniprepped plasmids were then cotransformed into *E. coli*
381 BTH101. Transformations were plated onto LB agar plates with kanamycin (50 μg/mL) and
382 carbenicillin (100 μg/mL) to select for transformants that received both plasmids. The resulting
383 strains were then grown up overnight in LB broth at 30°C, and 3 μL of the overnight culture was
384 spotted onto an LB agar plate supplemented with 500 μM IPTG, kanamycin (50 μg/mL),
385 carbenicillin (100 μg/mL), and 5-bromo-4-chloro-3-indolyl-β-d-galactopyranoside (X-gal)
386 (40 μg/mL). Plates were incubated at 30°C for 48 hours before imaging on an HP Scanjet
387 G4010 flatbed scanner.
388
389 **Electrophoretic mobility shift assays (EMSAs)**
390 Binding reactions contained 10 mM Tris·HCl pH 7.5, 1 mM EDTA, 10 mM KCl, 1 mM DTT, 50
391 μg/mL BSA, 0.1 mg/mL salmon sperm DNA, 5% glycerol, 3 nM DNA probe, and purified MBP-
392 ChiS cytoplasmic domain [4] at 25 nM, 50 nM, 100 nM, 200 nM, 400 nM, and 800 nM
393 concentrations (diluted in 10 mM Tris pH 7.5, 10 mM KCl, 1 mM DTT, and 5% glycerol). Binding
394 reactions were incubated in the dark at room temperature for 20 minutes before being loaded
395 into a 0.5X Tris Borate EDTA (TBE) polyacrylamide gel. Gels were run in 0.5X TBE buffer at
396 4°C, then imaged for Cy5 fluorescence on a ProteinSimple FluorChem R system.
397 Cy5-labeled DNA probes were made by Taq PCR with 4.34 μM Cy5-dCTP. Unlabeled probes
398 were made by Phusion PCR.
399
400 **Fluorescence reporter assays**
401 Strains were grown overnight in LB broth, supplemented with 1 μM IPTG and/or 50 ng/mL ATc
402 when applicable, at 30°C rolling. Then, overnight cultures were washed and resuspended in IO.
403 1 mL chitin reactions were made by mixing 10^8 cells (suspended in 100 μL IO), 150 μL of chitin
404 slurry (8g/150mL), 750 μL IO, and 1 μM IPTG and/or 50 ng/mL ATc when applicable. Chitin
405 reactions were incubated at 30°C shaking for 24 hours. Next, reactions were vortexed to
406 dislodge the cells from the chitin. The supernatants (containing the resuspended cells) were

407 then centrifuged, resuspended in IO, and placed on a glass coverslip beneath a 0.2% IO gelzan
408 pad. Cells were then imaged using mCherry, YFP, and CFP filter cubes. Image analysis was
409 performed to quantify the average fluorescence per cell in each channel. The background
410 fluorescence was determined in each channel by imaging and analyzing a non-fluorescent
411 strain, which was then subtracted from all samples. Reporter fluorescence (GFP or mCherry)
412 was then divided by the fluorescence of the CFP channel to normalize against the constitutively
413 expressed mTFP1 construct. The geometric mean was then calculated from 300 individual cells
414 for each replicate.
415
416 **Western blotting**
417 Strains were grown overnight in LB broth, supplemented with 1 μM IPTG when applicable, at
418 30°C rolling. Overnight cultures were then washed and resuspended in IO. For +chitin samples,
419 50 mL reactions were set up in flasks with $5x10^8$ cells (suspended in 5 mL IO), 7.5 mL of chitin
420 slurry, 37.5 mL IO, and 1 μM IPTG when applicable. For -chitin samples, 50 mL reactions were
421 set up in flasks with $5x10^8$ cells (suspended in 5 mL IO), 45 mL IO, and 1 μM IPTG when
422 applicable. Flasks were incubated at 30°C shaking for 24 hours. Cells were then dislodged from
423 chitin by vortexing. The supernatants (containing the resuspended cells) were then centrifuged,
424 washed, and resuspended in IO. Cells were then mixed 1:1 with 2X SDS-PAGE sample buffer
425 (200 mM Tris pH 6.8, 25% glycerol, 3.85% SDS, 0.02% Bromophenol Blue, 5% β-
426 mercaptoethanol) and boiled for 10 minutes. To blot for TfoS-FLAG, 4 μL of each sample was
427 separated on a 7.5% SDS-PAGE gel. To blot for RpoA, 2 μL of each sample was separated on a
428 15% SDS-PAGE gel. Following SDS-PAGE, the proteins were transferred to a polyvinylidene
429 difluoride (PVDF) membrane by electrophoresis, and then membranes were blocked for 1 hour
430 in 2% milk. Next, membranes were incubated rocking at room temperature overnight with
431 primary antibody: rabbit polyclonal anti-FLAG (Sigma) or mouse monoclonal anti-RpoA
432 (Biolegend). Membranes were then washed and incubated with either anti-mouse or anti-rabbit
433 horseradish peroxidase-conjugated secondary antibody for one hour rocking at room
434 temperature. Then, blots were washed, developed with Pierce ECL Western blotting substrate,
435 and imaged with a ProteinSimple FluorChem R system.
436
437 **Chromatin immunoprecipitation assays**
438 Chromatin Immunoprecipitation (ChIP) assays were performed exactly as previously described
439 [32]. *V. cholerae* strains were initiated from freezer stocks and incubated at 30°C in LB broth
440 rolling for ~16 hours. The following day, cultures were subcultured into fresh LB to an OD_{600} of
441 0.08 and incubated rolling for 6 hours at 30°C. Cells were incubated with 1% paraformaldehyde
442 at room temperature for 20 minutes shaking to crosslink DNA and proteins. A 1.2 molar excess
443 of Tris (10 minutes, room temperature, shaking) was used to quench residual
444 paraformaldehyde. Crosslinked cells were washed twice with TBS (25 mM Tris HCl, pH 7.5 and
445 125 mM NaCl) and then frozen at -80°C. Cells were then resuspended in lysis buffer (1x
446 FastBreak cell lysis reagent (Promega), 50 μg/mL lysozyme, 1% Triton X-100, 1 mM PMSF, and
447 1x protease inhibitor cocktail; 100x inhibitor cocktail contained the following: 0.07 mg/mL
448 phosphoramidon (Santa Cruz), 0.006 mg/mL bestatin (MPbiomedicals/Fisher Scientific), 1.67
449 mg/mL AEBSF (Gold Bio), 0.07 mg/mL pepstatin A (DOT Scientific), 0.07 mg/mL E64 (Gold Bio)
450 suspended in DMSO) to an OD_{600} of 50.0. These resuspensions were incubated rocking at room
451 temperature for 20 minutes to permit cell lysis. Lysates were then sonicated to shear DNA into
452 200-300bp fragments (sonication was performed with a Fisherbrand Model 705 Sonic
453 Dismembrator 6 times for 10 seconds at 1% amplitude, resting on ice for at least 30 seconds
454 between each sonication). The sonicated lysates were then clarified by centrifugation and
455 diluted 1:5 in Immunoprecipitation (IP) Buffer (50 mM HEPES NaOH pH 7.5, 150 mM NaCl, 1

mM EDTA, and 1% Triton X-100). An “input DNA” sample was collected from this diluted lysate. 1 mL of this diluted lysate was then added to Pierce anti-DYKDDDDK magnetic agarose equilibrated in IP buffer and then incubated at room temperature with end-over-end mixing. After two hours of incubation, a magnetic separation rack was used to facilitate removal of the supernatant. The agarose was washed twice with IP Buffer for 1 minute, once with Wash Buffer 1 (50 mM HEPES NaOH pH 7.5, 1 mM EDTA, 1% Triton X-100, 500 mM NaCl, and 0.1% SDS) for 5 minutes, once with Wash Buffer 2 (10 mM Tris HCl pH 8.0, 250 mM LiCl, 1 mM EDTA, 0.5% NP- 40, and 1% Triton X-100) for 5 minutes, and once with Buffer TE (10 mM tris pH 8.0 and 1 mM EDTA) for 1 minute. SDS elution buffer (50 mM Tris HCl pH 7.5, 10 mM EDTA, and 1% SDS) was used to elute protein and DNA off the magnetic agarose (30 minutes at 65°C). Supernatant was collected and digested for 2 hours with 20 µg Proteinase K in SDS Elution Buffer at 42°C. 6 hours of incubation at 65°C was then used to reverse crosslinking. Both the input and the output samples were then purified to remove non-DNA components. The abundance of P_{tfoR} in the input DNA (diluted 1:100) and output DNA was then quantified using quantitative PCR with iTaq Universal SYBR Green Supermix (Bio-Rad). A fold enrichment value was then generated by measuring the abundance of the *tfoR* promoter in the output (following immunoprecipitation) relative to the input (prior to immunoprecipitation). A locus that is not bound by ChiS or TfoS (*rpoB*) was used to normalize for total amount of DNA in the sample.

Statistical Comparisons

All statistical comparisons were made in Graphpad Prism and the statistical tests used are indicated in figure legends. For summary statistics and a complete list of all statistical comparisons, see **S1 Dataset**.

ACKNOWLEDGEMENTS

This work was supported by grant R35GM128674 from the National Institutes of Health to ABD.

REFERENCES

1. Demey LM, Gumerov VM, Xing J, Zhulin IB, DiRita VJ. Transmembrane Transcription Regulators Are Widespread in Bacteria and Archaea. Microbiol Spectr. 2023;11(3):e0026623. Epub 20230508. doi: 10.1128/spectrum.00266-23. PubMed PMID: 37154724; PubMed Central PMCID: PMCPMC10269533.

2. Brameyer S, Rösch TC, El Andari J, Hoyer E, Schwarz J, Graumann PL, Jung K. DNA-binding directs the localization of a membrane-integrated receptor of the ToxR family. Commun Biol. 2019;2:4. Epub 20190104. doi: 10.1038/s42003-018-0248-7. PubMed PMID: 30740540; PubMed Central PMCID: PMCPMC6320335.

3. Kaval KG, Chimalapati S, Siegel SD, Garcia N, Jaishankar J, Dalia AB, Orth K. Membrane-localized expression, production and assembly of Vibrio parahaemolyticus T3SS2 provides evidence for transertion. Nat Commun. 2023;14(1):1178. Epub 20230302. doi: 10.1038/s41467-023-36762-z. PubMed PMID: 36859532; PubMed Central PMCID: PMCPMC9977878.

4. Klancher CA, Yamamoto S, Dalia TN, Dalia AB. ChiS is a noncanonical DNA-binding hybrid sensor kinase that directly regulates the chitin utilization program in Vibrio cholerae. Proceedings of the National Academy of Sciences. 2020;117(33):20180-9. doi: 10.1073/pnas.2001768117.

5. Haas BL, Matson JS, DiRita VJ, Biteen JS. Single-molecule tracking in live Vibrio cholerae reveals that ToxR recruits the membrane-bound virulence regulator TcpP to the toxT promoter.

Mol Microbiol. 2015;96(1):4-13. Epub 20141104. doi: 10.1111/mmi.12834. PubMed PMID: 25318589; PubMed Central PMCID: PMCPMC6025817.

6. Calkins AL, Demey LM, Karslake JD, Donarski ED, Biteen JS, DiRita VJ. Independent Promoter Recognition by TcpP Precedes Cooperative Promoter Activation by TcpP and ToxR. mBio. 2021;12(5):e0221321. Epub 20210907. doi: 10.1128/mBio.02213-21. PubMed PMID: 34488449; PubMed Central PMCID: PMCPMC8546550.

7. Canals A, Pieretti S, Muriel-Masanes M, El Yaman N, Plecha SC, Thomson JJ, et al. ToxR activates the Vibrio cholerae virulence genes by tethering DNA to the membrane through versatile binding to multiple sites. Proc Natl Acad Sci U S A. 2023;120(29):e2304378120. Epub 20230710. doi: 10.1073/pnas.2304378120. PubMed PMID: 37428913; PubMed Central PMCID: PMCPMC10629549.

8. Yamamoto S, Mitobe J, Ishikawa T, Wai SN, Ohnishi M, Watanabe H, Izumiya H. Regulation of natural competence by the orphan two-component system sensor kinase ChiS involves a non-canonical transmembrane regulator in Vibrio cholerae. Molecular Microbiology. 2014;91(2):326-47. doi: https://doi.org/10.1111/mmi.12462.

9. Dalia AB, Lazinski DW, Camilli A. Identification of a Membrane-Bound Transcriptional Regulator That Links Chitin and Natural Competence in Vibrio cholerae. mBio. 2014;5(1):10.1128/mbio.01028-13. doi: 10.1128/mbio.01028-13.

10. Yamamoto S, Izumiya H, Mitobe J, Morita M, Arakawa E, Ohnishi M, Watanabe H. Identification of a chitin-induced small RNA that regulates translation of the tfoX gene, encoding a positive regulator of natural competence in Vibrio cholerae. J Bacteriol. 2011;193(8):1953-65. Epub 2011/02/15. doi: JB.01340-10 [pii]
10.1128/JB.01340-10. PubMed PMID: 21317321; PubMed Central PMCID: PMC3133033.

11. Lo Scrudato M, Blokesch M. The regulatory network of natural competence and transformation of Vibrio cholerae. PLoS Genet. 2012;8(6):e1002778. Epub 2012/06/28. doi: 10.1371/journal.pgen.1002778
PGENETICS-D-12-00108 [pii]. PubMed PMID: 22737089; PubMed Central PMCID: PMC3380833.

12. Seitz P, Blokesch M. DNA-uptake machinery of naturally competent Vibrio cholerae. Proc Natl Acad Sci U S A. 2013;110(44):17987-92. Epub 2013/10/16. doi: 1315647110 [pii]
10.1073/pnas.1315647110. PubMed PMID: 24127573.

13. Li X, Roseman S. The chitinolytic cascade in Vibrios is regulated by chitin oligosaccharides and a two-component chitin catabolic sensor/kinase. Proc Natl Acad Sci U S A. 2004;101(2):627-31. Epub 2003/12/31. doi: 10.1073/pnas.0307645100
0307645100 [pii]. PubMed PMID: 14699052; PubMed Central PMCID: PMC327198.

14. Meibom KL, Li XB, Nielsen AT, Wu CY, Roseman S, Schoolnik GK. The Vibrio cholerae chitin utilization program. Proc Natl Acad Sci U S A. 2004;101(8):2524-9. Epub 2004/02/26. doi: 101/8/2524 [pii]. PubMed PMID: 14983042; PubMed Central PMCID: PMC356983.

15. Klancher CA, Hayes CA, Dalia AB. The nucleoid occlusion protein SlmA is a direct transcriptional activator of chitobiose utilization in Vibrio cholerae. PLoS Genet.

2017;13(7):e1006877. doi: 10.1371/journal.pgen.1006877. PubMed PMID: 28683122; PubMed Central PMCID: PMCPMC5519180.

16. Davis JH, Rubin AJ, Sauer RT. Design, construction and characterization of a set of insulated bacterial promoters. Nucleic Acids Res. 2011;39(3):1131-41. Epub 20100915. doi: 10.1093/nar/gkq810. PubMed PMID: 20843779; PubMed Central PMCID: PMCPMC3035448.

17. Lim HC, Bernhardt TG. A PopZ-linked apical recruitment assay for studying protein-protein interactions in the bacterial cell envelope. Mol Microbiol. 2019;112(6):1757-68. Epub 2019/09/25. doi: 10.1111/mmi.14391. PubMed PMID: 31550057; PubMed Central PMCID: PMCPMC7218919.

18. Borgeaud S, Metzger LC, Scrignari T, Blokesch M. The type VI secretion system of Vibrio cholerae fosters horizontal gene transfer. Science. 2015;347(6217):63-7. doi: 10.1126/science.1260064. PubMed PMID: 25554784.

19. Molina-Quiroz RC, Dalia TN, Camilli A, Dalia AB, Silva-Valenzuela CA. Prophage-Dependent Neighbor Predation Fosters Horizontal Gene Transfer by Natural Transformation. mSphere. 2020;5(6). Epub 2020/11/13. doi: 10.1128/mSphere.00975-20. PubMed PMID: 33177216; PubMed Central PMCID: PMCPMC7657591.

20. Krukonis ES, Yu RR, Dirita VJ. The Vibrio cholerae ToxR/TcpP/ToxT virulence cascade: distinct roles for two membrane-localized transcriptional activators on a single promoter. Mol Microbiol. 2000;38(1):67-84. doi: 10.1046/j.1365-2958.2000.02111.x. PubMed PMID: 11029691.

21. Crawford JA, Krukonis ES, DiRita VJ. Membrane localization of the ToxR winged-helix domain is required for TcpP-mediated virulence gene activation in Vibrio cholerae. Mol Microbiol. 2003;47(5):1459-73. doi: 10.1046/j.1365-2958.2003.03398.x. PubMed PMID: 12603748.

22. Kinch LN, Cong Q, Jaishankar J, Orth K. Co-component signal transduction systems: Fast-evolving virulence regulation cassettes discovered in enteric bacteria. Proc Natl Acad Sci U S A. 2022;119(24):e2203176119. Epub 2022/06/02. doi: 10.1073/pnas.2203176119. PubMed PMID: 35648808; PubMed Central PMCID: PMCPMC9214523.

23. Martini L, Brameyer S, Hoyer E, Jung K, Gerland U. Dynamics of chromosomal target search by a membrane-integrated one-component receptor. PLoS Comput Biol. 2021;17(2):e1008680. Epub 20210204. doi: 10.1371/journal.pcbi.1008680. PubMed PMID: 33539417; PubMed Central PMCID: PMCPMC7888679.

24. Stracy M, Schweizer J, Sherratt DJ, Kapanidis AN, Uphoff S, Lesterlin C. Transient non-specific DNA binding dominates the target search of bacterial DNA-binding proteins. Mol Cell. 2021;81(7):1499-514 e6. Epub 20210222. doi: 10.1016/j.molcel.2021.01.039. PubMed PMID: 33621478; PubMed Central PMCID: PMCPMC8022225.

25. Miller VL, DiRita VJ, Mekalanos JJ. Identification of toxS, a regulatory gene whose product enhances toxR-mediated activation of the cholera toxin promoter. J Bacteriol. 1989;171(3):1288-93. doi. PubMed PMID: 2646275; PubMed Central PMCID: PMC209743.

606 26. Dalia AB. Natural Cotransformation and Multiplex Genome Editing by Natural
607 Transformation (MuGENT) of Vibrio cholerae. Methods Mol Biol. 2018;1839:53-64. doi:
608 10.1007/978-1-4939-8685-9_6. PubMed PMID: 30047054.
609
610 27. Dalia TN, Chlebek JL, Dalia AB. A modular chromosomally integrated toolkit for ectopic gene
611 expression in Vibrio cholerae. Sci Rep. 2020;10(1):15398. doi: 10.1038/s41598-020-72387-8.
612 PubMed PMID: 32958839; PubMed Central PMCID: PMCPMC7505983.
613
614 28. Dalia TN, Hayes CA, Stolyar S, Marx CJ, McKinlay JB, Dalia AB. Multiplex Genome Editing
615 by Natural Transformation (MuGENT) for Synthetic Biology in Vibrio natriegens. ACS Synth Biol.
616 2017;6(9):1650-5. doi: 10.1021/acssynbio.7b00116. PubMed PMID: 28571309.
617
618 29. Bartlett TM, Bratton BP, Duvshani A, Miguel A, Sheng Y, Martin NR, et al. A Periplasmic
619 Polymer Curves Vibrio cholerae and Promotes Pathogenesis. Cell. 2017;168(1-2):172-85 e15.
620 Epub 2017/01/14. doi: 10.1016/j.cell.2016.12.019. PubMed PMID: 28086090; PubMed Central
621 PMCID: PMCPMC5287421.
622
623 30. Ducret A, Quardokus EM, Brun YV. MicrobeJ, a tool for high throughput bacterial cell
624 detection and quantitative analysis. Nat Microbiol. 2016;1(7):16077. doi:
625 10.1038/nmicrobiol.2016.77. PubMed PMID: 27572972; PubMed Central PMCID:
626 PMCPMC5010025.
627
628 31. Schindelin J, Arganda-Carreras I, Frise E, Kaynig V, Longair M, Pietzsch T, et al. Fiji: an
629 open-source platform for biological-image analysis. Nat Methods. 2012;9(7):676-82. Epub
630 2012/06/30. doi: 10.1038/nmeth.2019. PubMed PMID: 22743772; PubMed Central PMCID:
631 PMCPMC3855844.
632
633 32. Green VE, Klancher CA, Yamamoto S, Dalia AB. The molecular mechanism for carbon
634 catabolite repression of the chitin response in Vibrio cholerae. PLoS Genet.
635 2023;19(5):e1010767. Epub 2023/05/12. doi: 10.1371/journal.pgen.1010767. PubMed PMID:
636 37172034; PubMed Central PMCID: PMCPMC10208484.
637
638

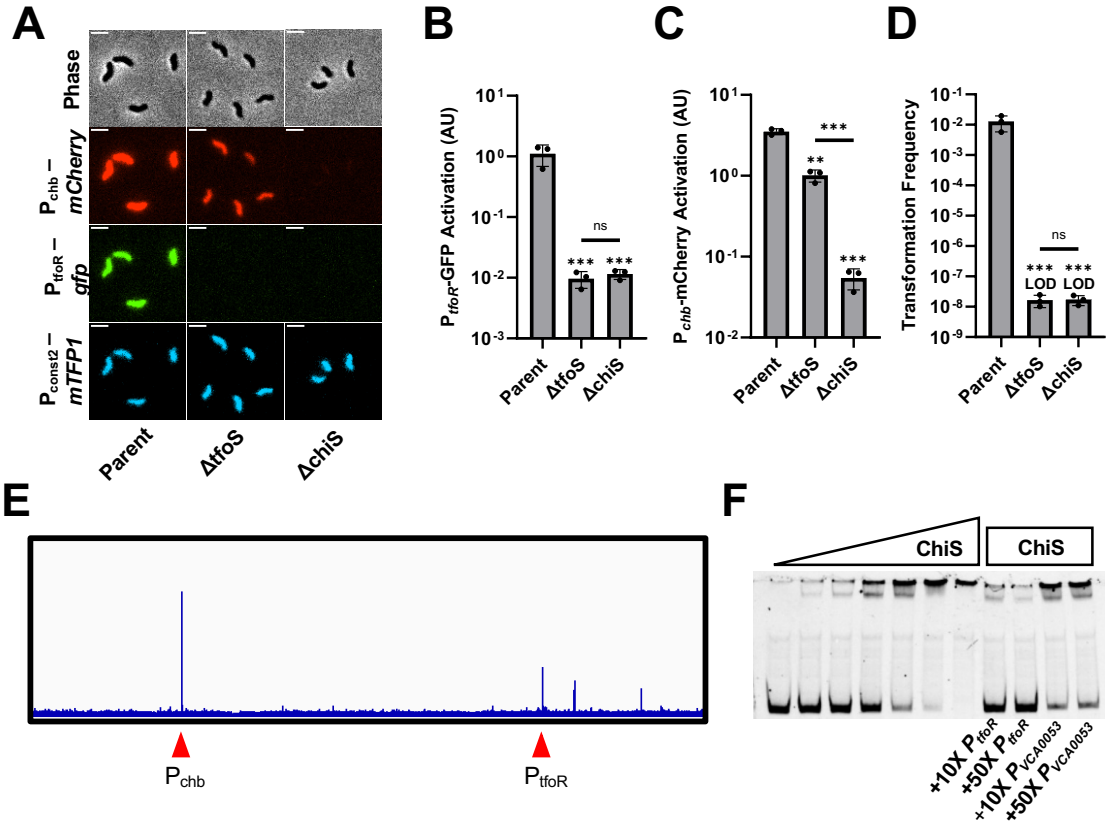

Fig. 1. *ChiS binds P_{tfoR} and is necessary for P_{tfoR} activation.* (**A-D**) Transcriptional reporter assays to assess chitin-dependent gene expression. The indicated strains all harbored 3 fluorescent reporter constructs: P_{chb}-*mCherry*, P_{tfoR}-*gfp*, and P_{const2}-*mTFP1*. Cells were incubated on chitin and then imaged via epifluorescence microscopy to assess reporter expression. Representative images are shown in **A** and the quantification of the results are shown in **B** and **C**. For each replicate (n = 3), the geometric mean fluorescence was determined by analyzing 300 individual cells. (**D**) Chitin-induced natural transformation assay of the indicated strains. Results are from three independent biological replicates and shown as the mean ± SD. Statistical comparisons in **B**, **C**, and **D** were made by one-way ANOVA with Tukey's multiple comparison test on log-transformed data. Statistical identifiers directly above bars represent comparisons to the parent. ns, not significant. *** = $p < 0.001$, ** = $p < 0.01$. LOD, limit of detection. (**E**) ChIP-seq analysis uncovers ChiS binding sites. The panel shows the mapping distribution of the ChIP-enriched DNA normalized to the mapping distribution of input DNA. ChIP peaks at the P_{chb} and P_{tfoR} loci are denoted by a red arrow. (**F**) EMSAs to test ChiS binding at P_{tfoR}. Increasing concentrations of the purified ChiS cytoplasmic domain (from left to right: 0 nM, 25 nM, 50 nM, 100 nM, 200 nM, 400 nM, 800 nM) were incubated with Cy5-labeled P_{tfoR} DNA probe. Cold competitor EMSAs were carried out using 200 nM ChiS and either 10-fold or 50-fold excess of the unlabeled competitor DNA probe as indicated. Data in **F** are representative of three independent experiments.

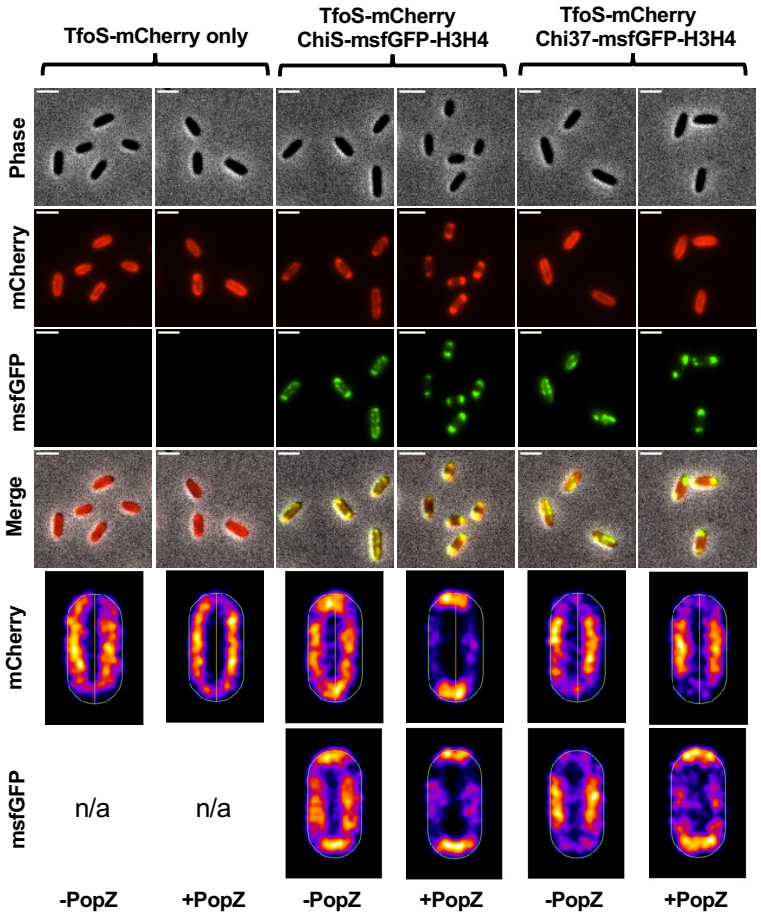

Fig. 2. *ChiS interacts with TfoS.* POLAR assays were conducted to assess the interaction between ChiS and TfoS. Colocalization was assessed in cells containing P_{bad}-*popZ* and the indicated ChiS and TfoS fusion constructs. The localization of these constructs was assessed in the absence (-PopZ) and presence (+PopZ) of PopZ induction. Scale bar, 2μm. Representative images of cells are shown along with heat maps that represent the fluorescence localization in 300 cells. Data are representative of three independent biological replicates. n/a, not applicable

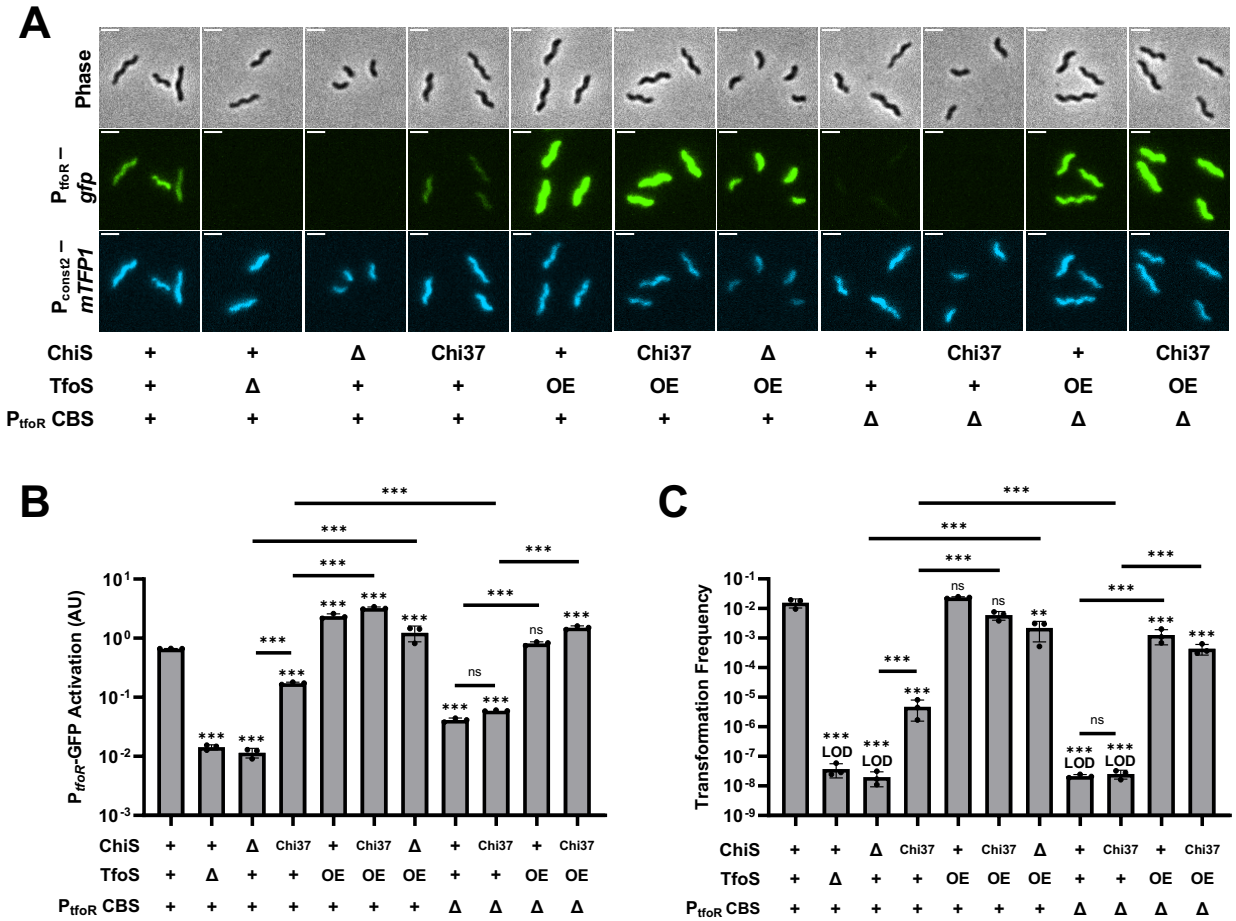

Fig. 3. *ChiS binding at P_{tfoR} is critical for activation when TfoS is expressed at native levels.* Strains harbored P_{tfoR}-*gfp,* P_{const2}-*mTFP1*, and the indicated mutations. Cells were incubated on chitin and then imaged via epifluorescence microscopy to assess reporter expression. For ChiS genotypes, "+" denotes that cells have a WT copy of ChiS, "Δ" denotes that cells lack ChiS, and "Chi37" indicates that cells express the Chi37 chimera instead of ChiS. For TfoS, "+" denotes $TfoS^{WT}$, "Δ" denotes that TfoS is deleted, and "OE" denotes that TfoS is overexpressed (P_{tac}-*tfoS* + 1μM IPTG). For P_{tfoR} CBS, "+" denotes the full-length wildtype P_{tfoR} promoter while "Δ" denotes $P_{tfoR}^{\Delta CBS}$. (**A**) Representative images of cells. Scale bar, 2μm. (**B**) Quantification of P_{tfoR}-*gfp* reporter activity. For each replicate (n = 3), the geometric mean fluorescence was determined by analyzing 300 individual cells. (**C**) Chitin-dependent transformation assays of the indicated strains. The mutations in P_{tfoR} were present in the P_{tfoR}-*gfp* reporter construct for transcriptional reporter assays, but at the native locus for transformation assays. Results are from three independent biological replicates and shown as the mean ± SD. Statistical comparisons in **B** and **C** are made by one-way ANOVA with Tukey's multiple comparison test on the log-transformed data. Statistical identifiers directly above bars represent comparisons to the parent. ns, not significant. *** = $p < 0.001$, ** = $p < 0.01$. LOD, limit of detection.

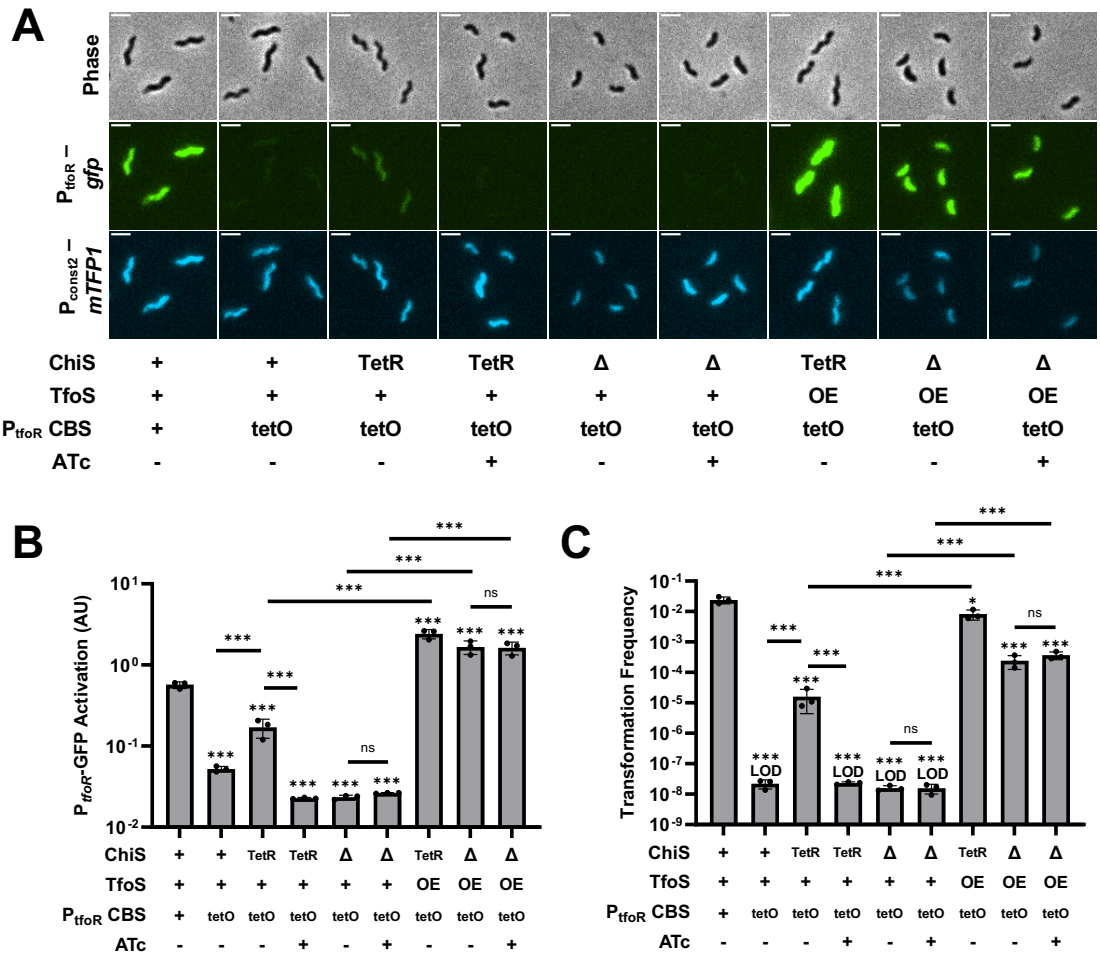

Fig. 4. *Recruitment of P_{tfoR} to the membrane is sufficient for TfoS-dependent activation.* Strains harbored P_{tfoR}-*gfp,* P_{const2}-*mTFP1*, and the indicated mutations. Cells were incubated on chitin and then imaged via epifluorescence microscopy to assess reporter expression. For ChiS genotypes, "+" denotes that cells have a WT copy of ChiS, "Δ" denotes that cells lack ChiS, and "TetR" indicates that cells express a $ChiS^{\Delta DBD}$-TetR fusion. For TfoS, "+" denotes $TfoS^{WT}$, "Δ" denotes that TfoS is deleted, and "OE" denotes that TfoS is overexpressed (P_{tac}-*tfoS* + 1μM IPTG). For P_{tfoR} CBS, "+" denotes the full-length wildtype P_{tfoR} promoter while "tetO" denotes $P_{tfoR}^{\Delta CBS::tetO}$. Where indicated, 50 ng/mL ATc was added to the reaction. (**A**) Representative images of cells. Scale bar, 2μm. (**B**) Quantification of P_{tfoR}-*gfp* reporter activity. For each replicate (n = 3), the geometric mean fluorescence was determined by analyzing 300 individual cells. (**C**) Chitin-dependent transformation assays of the indicated strains. The mutations in P_{tfoR} were present in the P_{tfoR}-*gfp* reporter construct for transcriptional reporter assays, but at the native locus for transformation assays. Results are from three independent biological replicates and shown as the mean ± SD. Statistical comparisons in **B** and **C** are made by one-way ANOVA with Tukey's multiple comparison test on the log-transformed data. Statistical identifiers directly above bars represent comparisons to the parent. ns, not significant. *** = $p < 0.001$, ** = $p < 0.01$. LOD, limit of detection.

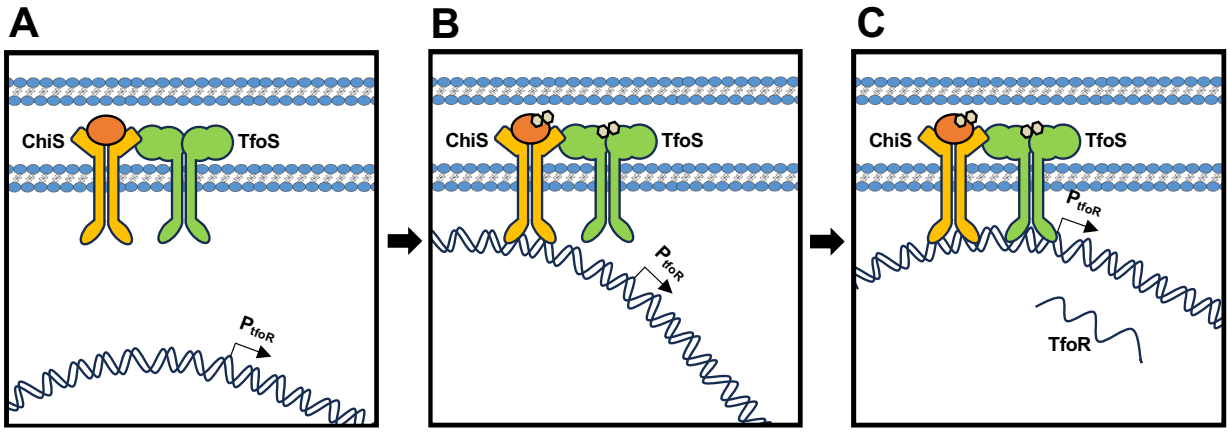

Fig. 5. *Proposed model for chitin-induced activation of P_{tfoR}.* (**A**) In the absence of chitin oligosaccharides, ChiS and TfoS are inactive. In the presence of chitin, (**B**) ChiS and TfoS are activated and ChiS binds upstream of the *tfoR* promoter. ChiS binds to TfoS to enhance its local concentration in the vicinity of membrane localized P_{tfoR}. (**C**) These combined activities of ChiS allow TfoS to subsequently bind P_{tfoR} and activate transcription of the *tfoR* small RNA that is critical for chitin-induced natural transformation.

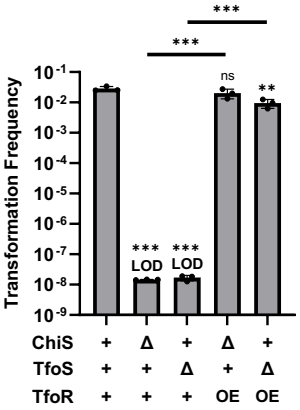

Fig. S1. *Overexpression of tfoR recovers transformation in ΔchiS and ΔtfoS backgrounds.* Chitin-dependent transformation assays of the indicated strains. For ChiS genotypes, "+" denotes that cells have a WT copy of ChiS and "Δ" denotes that cells lack ChiS. For TfoS genotypes, "+" denotes $TfoS^{WT}$ and "Δ" denotes that TfoS is deleted. For *tfoR*, "+" denotes WT *tfoR* and "OE" denotes that *tfoR* is overexpressed (P_{tac}-*tfoR* + 1μM IPTG). Results are from three independent biological replicates and shown as mean ± SD. Statistical comparisons are made by one-way ANOVA with Tukey's multiple comparison test on the log-transformed data. Statistical identifiers directly above bars represent comparisons to the parent. ns, not significant. *** = $p < 0.001$, ** = $p < 0.01$. LOD, limit of detection.

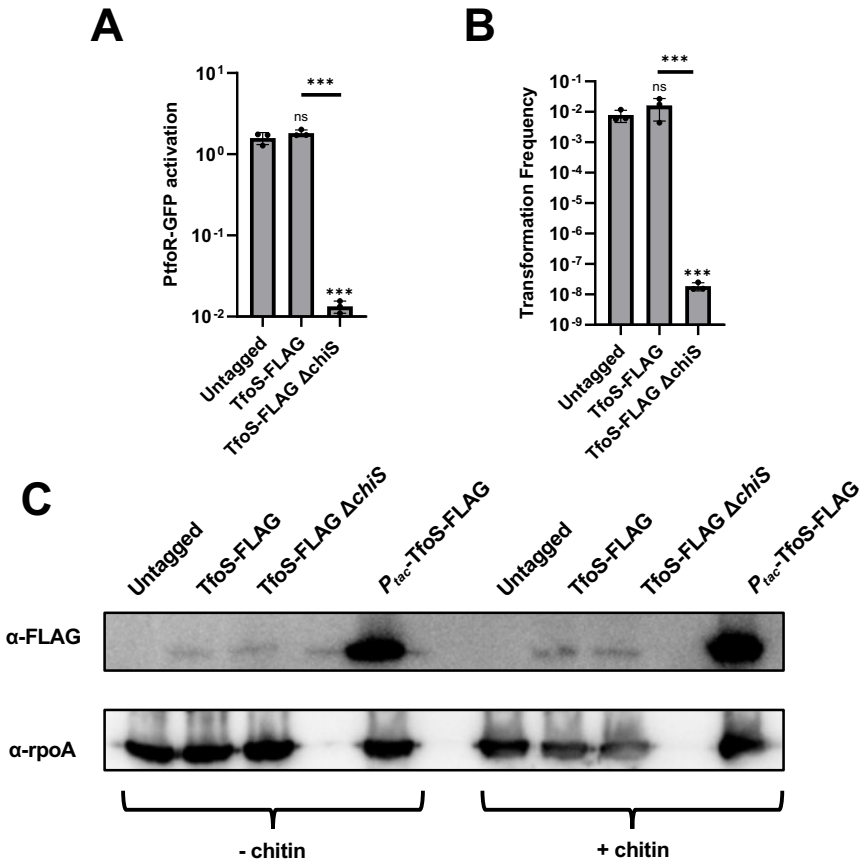

Fig. S2. *ChiS does not alter TfoS expression.* (**A**) Transcriptional reporter assays were performed by epifluorescence microscopy. The indicated strains all harbored P_{tfoR}-*gfp* and P_{const2}-*mTFP1* constructs. Cells were incubated on chitin for 24 hours and then imaged via epifluorescence microscopy to assess reporter expression. For each replicate (n = 3), the geometric mean fluorescence was determined by analyzing 300 individual cells. (**B**) Chitin-dependent transformation assays of indicated strains. Results are from three independent biological replicates and shown as the mean ± SD. Statistical comparisons in **A** and **B** were made by one-way ANOVA with Tukey's multiple comparison test. Statistical identifiers directly above bars represent comparisons to the parent. ns, not significant. *** = $p < 0.001$. LOD, limit of detection. (**C**) Western blot analysis of the indicated strains when cells were incubated with (+chitin) or without chitin (-chitin). Data are representative of two biological replicates.

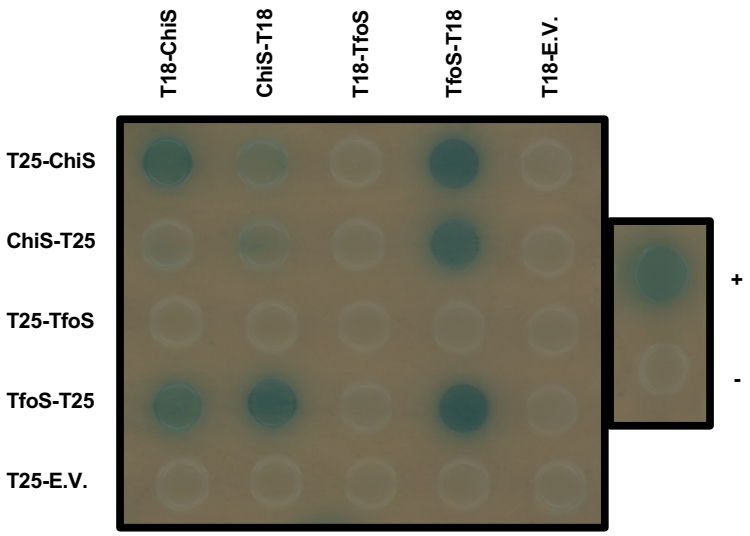

Fig. S3. *ChiS interacts with TfoS*. BACTH assess interactions between ChiS and TfoS. For BACTH assays, ChiS and TfoS either had an N-terminal fusion (indicated as TXX-protein) or a C-terminal fusion (indicated as protein-TXX) to the T25 or T18 fragment of adenylate cyclase.“+” and “-” indicate positive (T18-zip+T25-zip) and negative (T18 E.V. + T25 E.V.) controls for the assay. “E.V.” denotes an empty vector.

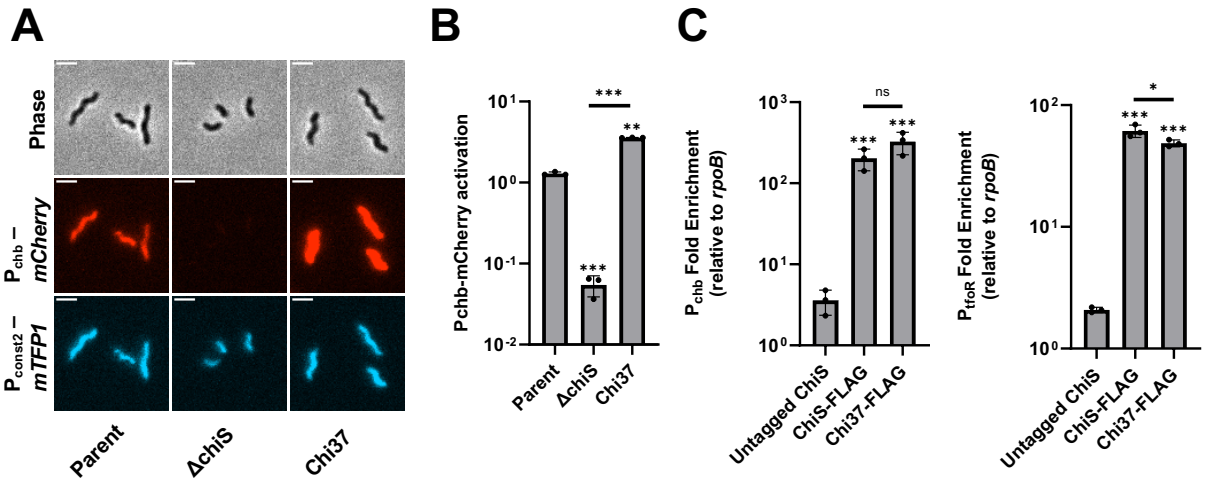

Fig. S4. *Chi37 is a functional chimera of ChiS*. (**A**-**B**) Transcriptional reporter assays were performed by epifluorescence microscopy. The indicated strains all harbored P_{chb}-*mCherry* and P_{const2}-*mTFP1* constructs. Cells were incubated on chitin for 24 hours and then imaged via epifluorescence microscopy to assess reporter expression. Representative images are shown in **A** and the quantification of the results are shown in **B**. For each replicate (n = 3), the geometric mean fluorescence was determined by analyzing 300 individual cells. (**C**) ChIP-qPCR assays were performed on the indicated strains to assess Chi37 binding at P_{chb} and P_{tfoR}. Results are from three independent biological replicates and shown as the mean ± SD. Statistical comparisons were made by one-way ANOVA with Tukey's multiple comparison test. Statistical identifiers directly above bars represent comparisons to the parent. ns, not significant. *** = $p < 0.001$, ** = $p < 0.01$.

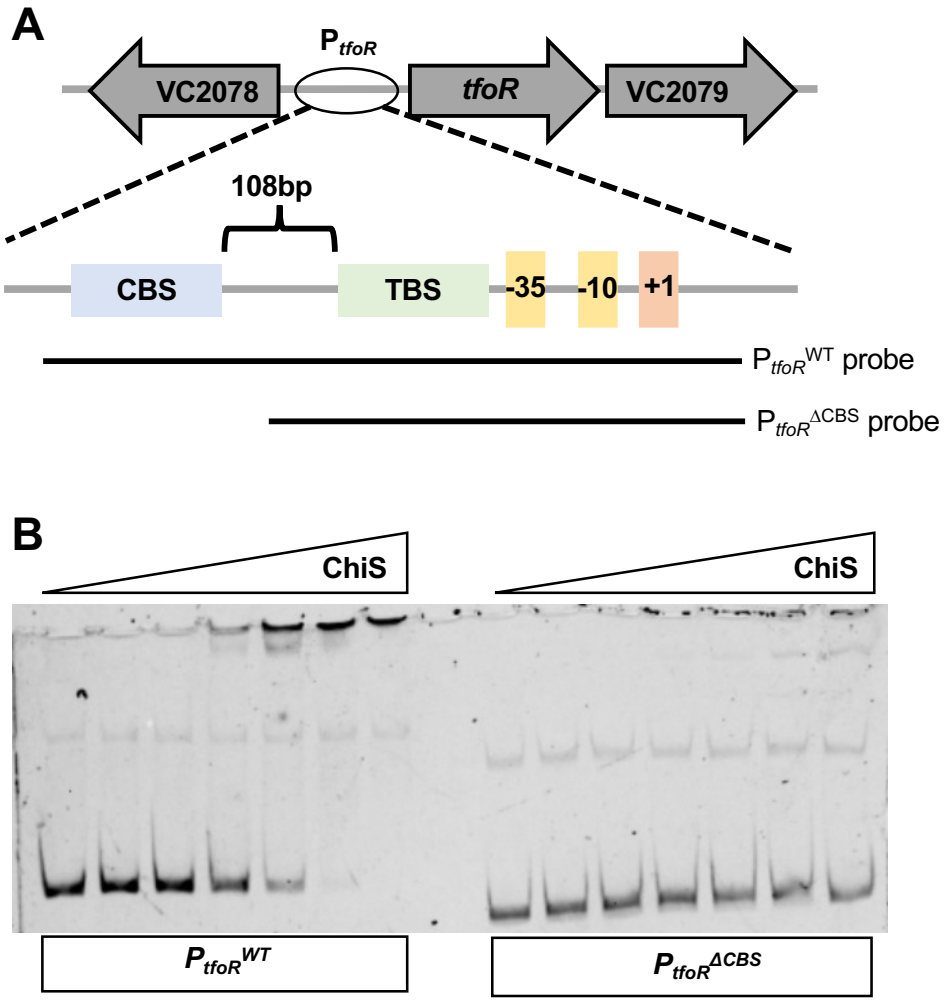

Fig. S5. *Truncating the 5' end of P_{tfoR} removes the ChiS binding site.* (**A**) Schematic of P_{tfoR}. The ChiS Binding Site (CBS) is located upstream of the TfoS Binding Site (TBS). The -35 and -10 elements are shown as yellow boxes, and the transcriptional start site is denoted as +1 in a red box. The sequences amplified to generate EMSA probes with (P_{tfoR}^{WT}) and without the CBS ($P_{tfoR}^{\Delta CBS}$) are also shown. (**B**) EMSAs of the purified ChiS cytoplasmic domain with the indicated probe DNA. Increasing concentrations of ChiS (from left to right: 0 nM, 25 nM, 50 nM, 100 nM, 200 nM, 400 nM, 800 nM) were incubated with the indicated Cy5-labelled P_{tfoR} DNA probe. P_{tfoR}^{WT} denotes the full-length wildtype P_{tfoR} promoter, while $P_{tfoR}^{\Delta CBS}$ denotes the truncated promoter where the ChiS binding site was removed from P_{tfoR}. Data are representative of three independent experiments.

769 **Table S1.** *Strains used in this study.*
770

Strain ID	Genotype	Reference in Manuscript
SAD030	*V. cholerae* WT E7946 Sm^R	Parent for all *V. cholerae* strains generated in this study Fig. S1 ChiS+ TfoS+ TfoR+
ACH0004	igVCA0265-66::$Spec^R$-P_{const2}-*mTFP1*; ΔVCA0692::Tm^R-P_{tfoR}-*gfp*; Δ*lacZ*::Kan^R-P_{chb}-*mCherry*	Fig. 1A-D Parent
ACH0014	igVCA0265-66::$Spec^R$-P_{const2}-*mTFP1*; ΔVCA0692::Tm^R-P_{tfoR}-*gfp*; Δ*lacZ*::Kan^R-P_{chb}-*mCherry*; Δ*tfoS*::Zeo^R	Fig. 1A-D ΔtfoS
ACH0019	igVCA0265-66::$Spec^R$-P_{const2}-*mTFP1*; ΔVCA0692::Tm^R-P_{tfoR}-*gfp*; Δ*lacZ*::Kan^R-P_{chb}-*mCherry*; Δ*chiS*::$Carb^R$	Fig. 1A-D, Fig. 3A-C, Fig. S3A-B ΔchiS / ΔchiS TfoS+ P_{tfoR} CBS+
ACH0205	Δ*crvA*::Zeo^R; igVCA0265-66::Cm^R-P_{bad}-*popZ*; Δ*lacZ*::$Spec^R$-P_{tac}-*tfoS*-L5-*mCherry*	Fig. 2 TfoS-mCherry only
ACH0204	Δ*crvA*::Zeo^R; igVCA0265-66::Cm^R-P_{bad}-*popZ*; Δ*lacZ*::$Spec^R$-P_{tac}-*tfoS*-L5-*mCherry*; ΔVCA0692::Tm^R-P_{tac}-*chiS-msfGFP*-H3H4	Fig. 2 TfoS-mCherry ChiS-msfGFP-H3H4
ACH0207	Δ*crvA*::Zeo^R; igVCA0265-66::Cm^R-P_{bad}-*popZ*; Δ*lacZ*::$Spec^R$-P_{tac}-*tfoS*-L5-*mCherry*; ΔVCA0692::Tm^R-P_{tac}-*chi37-msfGFP*-H3H4	Fig. 2 TfoS-mCherry Chi37-msfGFP-H3H4
ACH0142	igVCA0265-66::$Spec^R$-P_{const2}-*mTFP1*; ΔVCA0692::Tm^R-P_{tfoR}-*gfp*; Δ*lacZ*::Kan^R-P_{chb}-*mCherry*; Δ*chiS*::$Carb^R$; igVCA0587-88::Erm^R-P_{chiS}-*chiS*	Fig. 3A-C ; Fig. 4A-C ChiS+ TfoS+ P_{tfoR} CBS+
ACH0273	igVCA0265-66::$Spec^R$-P_{const2}-*mTFP1*; ΔVCA0692::Tm^R-P_{tfoR}-*gfp*; Δ*lacZ*::Kan^R-P_{chb}-*mCherry*; Δ*chiS*::$Carb^R$; igVCA0587-88::Erm^R-P_{chiS}-*chiS*; Δ*tfoS*::Zeo^R	Fig. 3A-C ChiS+ ΔtfoS P_{tfoR} CBS+
ACH0141	igVCA0265-66::$Spec^R$-P_{const2}-*mTFP1*; ΔVCA0692::Tm^R-P_{tfoR}-*gfp*; Δ*lacZ*::Kan^R-P_{chb}-*mCherry*; Δ*chiS*::$Carb^R$; igVCA0587-88::Erm^R-P_{chiS}-*chi37*	Fig. 3A-C Chi37 TfoS+ P_{tfoR} CBS+
ACH0144	igVCA0265-66::$Spec^R$-P_{const2}-*mTFP1*; ΔVCA0692::Tm^R-P_{tfoR}-*gfp*; Δ*chiS*::$Carb^R$; igVCA0587-88::Erm^R-P_{chiS}-*chiS*; Δ*lacZ*::Zeo^R-P_{tac}-*tfoS*	Fig. 3A-C ChiS+ TfoS OE P_{tfoR} CBS+
ACH0143	igVCA0265-66::$Spec^R$-P_{const2}-*mTFP1*; ΔVCA0692::Tm^R-P_{tfoR}-*gfp*; Δ*chiS*::$Carb^R$; igVCA0587-88::Erm^R-P_{chiS}-*chi37*; Δ*lacZ*::Zeo^R-P_{tac}-*tfoS*	Fig. 3A-C Chi37 TfoS OE P_{tfoR} CBS+
ACH0147	igVCA0265-66::$Spec^R$-P_{const2}-*mTFP1*; ΔVCA0692::Tm^R-P_{tfoR}-*gfp*; Δ*chiS*::$Carb^R$; Δ*lacZ*::Zeo^R-P_{tac}-*tfoS*	Fig. 3A-C ΔchiS TfoS OE P_{tfoR} CBS+
ACH0284	igVCA0265-66::$Spec^R$-P_{const2}-*mTFP1*; ΔVCA0692::Tm^R-$P_{tfoR}^{\Delta CBS}$-*gfp*; Δ*chiS*::$Carb^R$; igVCA0587-88::Erm^R-P_{chiS}-*chiS*	Fig. 3A-B ChiS+ TfoS+ ΔP_{tfoR} CBS

ACH0285	igVCA0265-66::Spec^R-P$_{const2}$-*mTFP1*; ΔVCA0692::Tm^R-P$_{tfoR}$ $^{\Delta CBS}$-*gfp*; Δ*chiS*::Carb^R; igVCA0587-88::Erm^R-P$_{chiS}$-*chiS*; Δ*lacZ*::Zeo^R-P$_{tac}$-*tfoS*	Fig. 3A-B ChiS+ TfoS OE ΔP$_{tfoR}$ CBS
ACH0274	igVCA0265-66::Spec^R-P$_{const2}$-*mTFP1*; ΔVCA0692::Tm^R-P$_{tfoR}$ $^{\Delta CBS}$-*gfp*; Δ*chiS*::Carb^R; igVCA0587-88::Erm^R-P$_{chiS}$-*chi37*	Fig. 3A-B Chi37 TfoS+ ΔP$_{tfoR}$ CBS
ACH0275	igVCA0265-66::Spec^R-P$_{const2}$-*mTFP1*; ΔVCA0692::Tm^R-P$_{tfoR}$ $^{\Delta CBS}$-*gfp*; Δ*chiS*::Carb^R; igVCA0587-88::Erm^R-P$_{chiS}$-*chi37*; Δ*lacZ*::Zeo^R-P$_{tac}$-*tfoS*	Fig. 3A-B Chi37 TfoS OE ΔP$_{tfoR}$ CBS
ACH0278	igVCA0265-66::Spec^R-P$_{const2}$-*mTFP1*; ΔVCA0692::Tm^R-P$_{tfoR}$-*gfp*; Δ*lacZ*::Kan^R-P$_{chb}$-*mCherry*; Δ*chiS*::Carb^R; igVCA0587-88::Erm^R-P$_{chiS}$-*chi37*; P$_{tfoR}$$^{\Delta CBS}$; ΔVC1807::Smx^R	Fig. 3C Chi37 TfoS+ ΔP$_{tfoR}$ CBS
ACH0279	igVCA0265-66::SpecR-P$_{const2}$-*mTFP1*; ΔVCA0692::TmR-P$_{tfoR}$-*gfp*; ΔlacZ::KanR-P$_{chb}$-*mCherry*; Δ*chiS*::CarbR; igVCA0587-88::ErmR-P$_{chiS}$-*chiS*; P$_{tfoR}$$^{\Delta CBS}$; ΔVC1807::SmxR	Fig. 3C ChiS+ TfoS+ ΔP$_{tfoR}$ CBS
ACH0280	igVCA0265-66::Spec^R-P$_{const2}$-*mTFP1*; ΔVCA0692::Tm^R-P$_{tfoR}$-*gfp*; Δ*chiS*::Carb^R; igVCA0587-88::Erm^R-P$_{chiS}$-*chi37*; P$_{tfoR}$$^{\Delta CBS}$; ΔVC1807::Smx^R; Δ*lacZ*::Zeo^R-P$_{tac}$-*tfoS*	Fig. 3C Chi37 TfoS OE ΔP$_{tfoR}$ CBS
ACH0281	igVCA0265-66::Spec^R-P$_{const2}$-*mTFP1*; ΔVCA0692::Tm^R-P$_{tfoR}$-*gfp*; Δ*chiS*::Carb^R; igVCA0587-88::Erm^R-P$_{chiS}$-*chiS*; P$_{tfoR}$$^{\Delta CBS}$; ΔVC1807::Smx^R; Δ*lacZ*::Zeo^R-P$_{tac}$-*tfoS*	Fig. 3C ChiS+ TfoS OE ΔP$_{tfoR}$ CBS
ACH0374	igVCA0265-66::Spec^R-P$_{const2}$-*mTFP1*; ΔVCA0692::Tm^R-P$_{tfoR}$$^{\Delta CBS::tetO}$-*gfp*; Δ*lacZ*::Kan^R-P$_{chb}$-*mCherry*; Δ*chiS*::Carb^R; igVCA0587-88::Erm^R-P$_{chiS}$-*chiS*	Fig. 4A-B ChiS+ TfoS+ P$_{tfoR}$ CBS tetO
ACH0310	igVCA0265-66::Spec^R-P$_{const2}$-*mTFP1*; ΔVCA0692::Tm^R-P$_{tfoR}$$^{\Delta CBS::tetO}$-*gfp*; Δ*lacZ*::Kan^R-P$_{chb}$-*mCherry*; Δ*chiS*::Carb^R; igVCA0587-88::Erm^R-P$_{chiS}$-*chiS*$^{\Delta DBD}$-*TetR*	Fig. 4A-B ChiS TetR TfoS+ P$_{tfoR}$ CBS tetO
ACH0325	igVCA0265-66::Spec^R-P$_{const2}$-*mTFP1*; ΔVCA0692::Tm^R-P$_{tfoR}$$^{\Delta CBS::tetO}$-*gfp*; Δ*lacZ*::Kan^R-P$_{chb}$-*mCherry*; Δ*chiS*::Carb^R	Fig. 4A-B ΔchiS TfoS+ P$_{tfoR}$ CBS tetO
ACH0338	igVCA0265-66::Spec^R-P$_{const2}$-*mTFP1*; ΔVCA0692::Tm^R-P$_{tfoR}$$^{\Delta CBS::tetO}$-*gfp*; Δ*chiS*::Carb^R; igVCA0587-88::Erm^R-P$_{chiS}$-*chiS*$^{\Delta DBD}$-*TetR*; Δ*lacZ*::Zeo^R-P$_{tac}$-*tfoS*	Fig. 4A-B ChiS TetR TfoS OE P$_{tfoR}$ CBS tetO
ACH0340	igVCA0265-66::Spec^R-P$_{const2}$-*mTFP1*; ΔVCA0692::Tm^R-P$_{tfoR}$$^{\Delta CBS::tetO}$-*gfp*; Δ*lacZ*::Kan^R-P$_{chb}$-*mCherry*; Δ*chiS*::Carb^R; Δ*lacZ*::Zeo^R-P$_{tac}$-*tfoS*	Fig. 4A-B ΔchiS TfoS OE P$_{tfoR}$ CBS tetO
ACH0401	Δ*chiS*::Carb^R; igVCA0587-88::Erm^R-P$_{chiS}$-*chiS*; P$_{tfoR}$$^{\Delta CBS::tetO}$; ΔVC1807::Smx^R	Fig. 4C ChiS+ TfoS+ P$_{tfoR}$ CBS tetO

ACH0399	Δ*chiS*::Carb^R; igVCA0587-88::Erm^R-P$_{chiS}$-*chiS*$^{\Delta DBD}$-*TetR*; P$_{tfoR}^{\Delta CBS::tetO}$; ΔVC1807::Smx^R	Fig. 4C ChiS TetR TfoS+ P$_{tfoR}$ CBS tetO
ACH0398	Δ*chiS*::Carb^R; P$_{tfoR}^{\Delta CBS::tetO}$; ΔVC1807::Smx^R	Fig. 4C ΔchiS TfoS+ P$_{tfoR}$ CBS tetO
ACH0400	Δ*chiS*::Carb^R; igVCA0587-88::Erm^R-P$_{chiS}$-*chiS*$^{\Delta DBD}$-*TetR*; P$_{tfoR}^{\Delta CBS::tetO}$; ΔVC1807::Smx^R; Δ*lacZ*::Zeo^R-P$_{tac}$-*tfoS*	Fig. 4C ChiS TetR TfoS OE P$_{tfoR}$ CBS tetO
ACH0418	Δ*chiS*::Carb^R; P$_{tfoR}^{\Delta CBS::tetO}$; ΔVC1807::Smx^R; Δ*lacZ*::Zeo^R-P$_{tac}$-*tfoS*	Fig. 4C ΔchiS TfoS OE P$_{tfoR}$ CBS tetO
ACH0288	Δ*chiS*::Carb^R	Fig. S1 ΔchiS TfoS+ TfoR+
ACH0289	Δ*tfoS*::Zeo^R	Fig. S1 ChiS+ ΔtfoS TfoR+
ACH0290	Δ*chiS*::Carb^R; Δ*lacZ*::Spec^R-P$_{tac}$-*tfoR*	Fig. S1 ΔchiS TfoS+ TfoR OE
ACH0291	Δ*tfoS*::Zeo^R; Δ*lacZ*::Spec^R-P$_{tac}$-*tfoR*	Fig. S1 ChiS+ ΔtfoS TfoR OE
ACH0186	igVCA0265-66::Spec^R-P$_{const2}$-*mTFP1*; Δ*lacZ*::Kan^R-P$_{tfoR}$-*gfp*; ΔVC1807::Cm^R	Fig. S2 Untagged
ACH0185	igVCA0265-66::Spec^R-P$_{const2}$-*mTFP1*; Δ*lacZ*::Kan^R-P$_{tfoR}$-*gfp*; ΔVC1807::Cm^R; *tfoS* N929 1X FLAG	Fig. S2 TfoS-FLAG
ACH0189	igVCA0265-66::Spec^R-P$_{const2}$-*mTFP1*; Δ*lacZ*::Kan^R-P$_{tfoR}$-*gfp*; ΔVC1807::Cm^R; *tfoS* N929 1X FLAG; Δ*chiS*::Carb^R	Fig. S2 TfoS-FLAG ΔchiS
ACH0286	igVCA0265-66::Spec^R-P$_{const2}$-*mTFP1*; ΔVC1807::Cm^R; Δ*lacZ*::Zeo^R-P$_{tac}$-*tfoS N929 1X FLAG*	Fig. S2 Ptac-TfoS-FLAG
ACH0031	TG1, pKT25-ChiS Kan^R	Fig. S3 T25-ChiS
ACH0035	TG1, pKT25-TfoS Kan^R	Fig. S3 T25-TfoS
VEG0253	TG1, pKNT25-ChiS Kan^R	Fig. S3 ChiS-T25
ACH0036	TG1, pKNT25-TfoS Kan^R	Fig. S3 TfoS-T25
ACH0033	TG1, pUT18C-ChiS Carb^R	Fig. S3 T18-ChiS
ACH0037	TG1, pUT18C-TfoS Carb^R	Fig. S3 T18-TfoS
ACH0034	TG1, pUT18-ChiS Carb^R	Fig. S3

		ChiS-T18
ACH0038	TG1, pUT18-TfoS Carb^R	Fig. S3 TfoS-T18
SAD2236	TG1, pKT25 vector Kan^R	Fig. S3 T25-E.V.
SAD2240	TG1, pUT18C vector Carb^R	Fig. S3 T18-E.V.
SAD2238	TG1, pKT25-zip Kan^R	Fig. S3 T25-zip
SAD2241	TG1, pUT18C-*zip* Carb^R	Fig. S3 T18-zip
VEG0565	Δ*lacZ*::Kan^R-P$_{chb}$-*gfp*; Δ*chiS/cbp*::Carb^R; ΔVCA0692::*Tm^R*-P$_{chiS}$-*chiS*	Fig. S4 Untagged ChiS
TND1801	Δ*lacZ*::Kan^R-P$_{chb}$-*gfp*; Δ*chiS/cbp*::Carb^R; ΔVCA0692::Tm^R-P$_{chiS}$-*chiS* 1X FLAG after E566	Fig. S4 ChiS-FLAG
CAK672	Δ*lacZ*::Kan^R-P$_{chb}$-*gfp*; Δ*chiS/cbp*::Carb^R; ΔVCA0692::Tm^R-P$_{chiS}$-*chi37* 3X FLAG	Fig. S4 Chi37-FLAG

771

772 **Table S2.** *Primers used in this study.*
773

Primers for SOE Deletions		
Primer	**Sequence**	**Description**
ABD123	ATTCCGGGGATCCGTCGAC	Antibiotic resistance cassette F
ABD124	TGTAGGCTGGAGCTGCTTC	Antibiotic resistance cassette R
ABD767	TTAATTTGGATCCCTGCGACACTC	ΔchiS F1 for Up arm
ABD768	gtcgacggatccccggaatCAAAAAACGTGAGGAGA ATGCC	ΔchiS R1 for Up arm
ABD769	gaagcagctccagcctacaTTCTTGAGCATTGCAAAG AAGC	ΔchiS F2 for Down arm
ABD770	CTGGAACGAATGAAGAAGTCCAG	ΔchiS R2 for Down arm
ABD640	GCAATACACGCTGTGTTTCACCG	ΔtfoS F1 for Up arm
ABD641	gtcgacggatccccggaatCAATTCAAGAATTCGTGCTTTATTGG	ΔtfoS R1 for Up arm
ABD642	gaagcagctccagcctacaTAATAGAGCCCATCTCTATTTCATC	ΔtfoS F2 for Down arm
ABD643	TCGTTTTCTAAGGCTCGAATCGCC	ΔtfoS R2 for Down arm
BBC1782	CAAGCGATGTACGAACGAAC	ΔcrvA F1 for Up arm
BBC1783	gtcgacggatccccggaatCCACATAAAGTGGGAAAGACAAAC	ΔcrvA R1 for Up arm
BBC1784	gaagcagctccagcctacaGTCAATGGCAATGACACGG	ΔcrvA F2 for Down arm
BBC1785	GCTTGACGTTGTTGCTTACTGG	ΔcrvA R2 for Down arm
BBC717	AAATAGATTTGGTGACTTTACCTCC	ΔVC1807 F1 for UP arm
ABD340	gtcgacggatccccggaatACGTTTCATTAGTCACCTCTATTGTTAA CTTGTTC	ΔVC1807 R1 for Up arm
ABD341	gaagcagctccagcctacaTAGTCGAAAATAAAAAAAAGAGGCTCG CCTC	ΔVC1807 F2 for Down arm
BBC2412	CAATTTTGCTTTTGGACCATCC	ΔVC1807 R2 for Down arm
ABD725	GAAGCAGCTCCAGCCTACA	Detect F for all deletions
CKP001	cccgggatcctgtgtgaaattgCTTATTTGGCCTTGTTTGATAATG	ΔchiS detect R
CKP682	AATAGTCAACGTCAATTCTGTC	ΔtfoS detect R
BBC1786	TTTTGTGATGGCTGGATGTCG	ΔcrvA detect R
BBC030	ACCAAACAATAAACGAGTAATGC	ΔVC1807 detect R
Primers for Reporter Constructs		
Primer	**Sequence**	**Description**
BBC3230	GCAGTAAATCCGACTTTGGAG	Insert construct at igVCA0265-66 F1
BBC3260	CCCGGGATCCTGTGTGAAATTG	igVCA0265-66 $Spec^R$ R1 for P_{const2}
BBC4271	caatttcacacaggatcccgggAGGAGGTtGTGTTATGGTGAGCAAA GGTG	Amplify mTFP1 F
BBC4272	tgtaggctggagctgcttcCTATTTATACAGTTCATCCATACCATC	Amplify mTFP1 R
CKP803	gaagcagctccagcctacaTCATAATTTAAGGCGTTAGCAG	Insert construct at igVCA0265-66 F2
BBC3231	TCTCATAAACCTCATGGTAGACG	Insert construct at igVCA0265-66 R2

BBC832	GCTTTTTGCTACAACGACCG	Insert construct at VCA0692 F1
BBC263	TACCGAGGACGCGAAGCTGCTCATTAGGCACCCCAGGC	Insert construct at VCA0692 R1
CKP699	cagcttcgcgtcctcggtaAATAGTCAACGTCAATTCTGTC	Amplify PtfoR-GFP F
BBC254	tgtaggctggagctgcttcTTAGTTGTATAGTTCATCCATGCC	Amplify PtfoR-GFP R
BBC830	gaagcagctccagcctacaGTTGAGTTGGATGCAGCACC	Insert construct at VCA0692 F2
BBC834	CACAATTTCTCGCTTAAAATGTCC	Insert construct at VCA0692 R2
BBC2511	CTCATTAGGCACCCCAGGC	PtfoR$^{\Delta CBS}$-GFP R1
BBC4082	gcctggggtgcctaatgagTAAAATCAACACCTTAAAAACATGATTAAGC	PtfoR$^{\Delta CBS}$-GFP F2
VGP0466	tctctatcactgatagggaTAgAATAGGTACTAATCAgAATAGTGAGGAG	PtfoR$^{\Delta CBS::tetO}$-GFP R1
VGP0467	tccctatcagtgatagagaTCACATTACCATTAAgATGTCAAACGG	PtfoR$^{\Delta CBS::tetO}$-GFP F2
VGP0468	ctcctcactattctgattagtacctattctaTCCCTATCAGTGATAGAGAttcttTCCCTATCAGTGATAGAGAttcttTCCCTATCAGTGATAGAGAatcgtTCCCTATCAGTGATAGAGAtcacattaccattaagatgtcaaacgg	4X tetO miniFRT F
VGP0469	ccgtttgacatcttaatggtaatgtgaTCTCTATCACTGATAGGGAacgatTCTCTATCACTGATAGGGAaagaaTCTCTATCACTGATAGGGAaagaaTCTCTATCACTGATAGGGAtagaataggtactaatcagaatagtgaggag	4X tetO miniFRT R
Primers for BACTH		
Primer	**Sequence**	**Description**
BBC2513	gaagcagctccagcctacaGATCCCCGGGTACCTAAGTAAC	Amplify BACTH pKT25 to make T25-XX vectors F
BBC2512	tccacctgctccacctgcCTCTAGAGTCGACCCTGCAG	Amplify BACTH pKT25 to make T25-XX vectors R
BBC2515	gaagcagctccagcctacaCCGAGCTCGAATTCATCGATATAAC	Amplify BACTH pUT18C to make T18-XX vectors F
BBC2514	tccacctgctccacctgcCTCTAGAGTCGACCTGCAG	Amplify BACTH pUT18C to make T18-XX vectors R
BBC2517	gcaggtggaagtggtggaGATCCCCGGGTACCGAGC	Amplify BACTH pKNT25 and pUT18 to make XX-T25 and XX-T18 vectors F
BBC2516	tccacctgctccacctgcCTCTAGAGTCGACCTGCAGG	Amplify BACTH pKNT25 and pUT18 to make XX-T25 and XX-T18 vectors R
BBC2762	gcaggtggagcaggtggaTTTAGGTTCTATCGAAAACAAAAATTC	BACTH TXX-ChiS or ChiS-TXX F
BBC3203	tgtaggctggagctgcttcTTATTCACTGGTCAGGAGTTTTTGC	BACTH TXX-ChiS R
BBC3204	tccaccacttccacctgcTTCACTGGTCAGGAGTTTTTGC	BACTH ChiS-TXX R
VGP0213	gcaggtggagcaggtggaTCGCTGACAGGGGAACTCG	BACTH TXX-TfoS or TfoS-TXX F
VGP0214	tgtaggctggagctgcttcTTAGTTTTCTTGATCTTCGATGAATTG	BACTH TXX-TfoS R

VEG0215	tccaccacttccacctgcGTTTTCTTGATCTTCGATGAATTGG	BACTH TfoS-TXX R
Primers for EMSAs		
Primer	**Sequence**	**Description**
BBC4084	gtcgacggatccccggaatCCGGTGATATTCTCATTTTAGC	P_{tfoR}^{WT} F from Fig. 1F
CKP235	gtcgacggatccccggaatCAAATATATCCTCCTCACTATTTTGATTAG	P_{tfoR}^{WT} and $P_{tfoR}^{\Delta CBS}$ F from Fig. S5
BBC929	AACATCACCATCTAATTCAACAAG	P_{tfoR}^{WT} and $P_{tfoR}^{\Delta CBS}$ R
CKP248	TGTACTGTACAAATATTTTTTTTGTACAG	$P_{VCA0053}$ F
CKP249	TGTGGGGTTGCCATGGTTAC	$P_{VCA0053}$ R
Primers for ChiS Constructs		
Primer	**Sequence**	**Description**
BBC4387	GATAACGATCGATAGCTGGTTGG	Insert construct at igVCA0587-88 F1
BBC647	tttttctatttctgaatcgattcatacgaCTCATTAGGCACCCCAGGC	igVCA0587-88 Erm^R R1
BBC1889	tcgtatgaatcgattcagaaatagaaaaaTTTGCCGCTTTTAACGTAAATCAG	Amplify PchiS-ChiS F
BBC577	tgtaggctggagctgcttcTTATTCACTGGTCAGGAGTTTTTGC	Amplify PchiS-ChiS R
BBC4384	gaagcagctccagcctacaGCAGTGTTGGCTGCAACTCC	Insert construct at igVCA0587-88 F2
BBC4388	ATCATGGTGCTGTTTAGTTGG	Insert construct at igVCA0587-88 R2
CAK311	ATTTTATGGCTGAATTTCATAATTAAGGTGTTACTTTCGGTG	Mlp37 periplasmic domain stitch to PchiS R1
CAK312	CCGAAAGTAACACCTTAATTATGAAATTCAGCCATAAAATTGTTG	Mlp37 periplasmic domain stitch to PchiS F
CKP384	GCGGTGAGGTAATGAAATTAACGATAAACAGTAGAACAAACACG	Mlp37 periplasmic domain R
CKP385	TTCTACTGTTTATCGTTAATTTCATTACCTCACCGCTTTTG	ChiS HAMP + cytoplasmic stitch to Mlp37 periplasmic F2
CKP397	ataatcaatgtcgtgatccttgtagtcaccatcatggtctttataatcATCGACAATCTCATCAACACTG	Mlp37 periplasmic domain truncation 3X FLAG R1
CKP396	ggtgactacaaggatcacgacattgattataaggatgacgatgacaaaGAATTTTTGGGTGAAAGCAAAATC	Mlp37 periplasmic domain truncation 3X FLAG F2
BBC4756	gccagctttcgcggcagcttcgccaccagaaccgctTTGATACTCGCCCGAGGCTT	Amplify $ChiS^{\Delta DBD}$ R1
BBC4757	agcggttctggtggcgaagctgccgcgaaagctggcGTGTCTAGATTAGATAAAAGTAAAGTG	Amplify TetR F
VGP0470	tgtaggctggagctgcttcTTAtccacctgctccacctgc	Amplify TetR R
Primers for POLAR Constructs		
Primer	**Sequence**	**Description**
ABD332	GGCTGAACGTGGTTGTCGAAAATGAC	Insert construct at *lacZ* F1
BBC3668	cagctttcgcggcagcttcgccaccagaaccgctGTTTTCTTGATCTTCGATGAATTGGC	Amplify TfoS R1

BBC3669	ttctggtggcgaagctgccgcgaaagctggcGTGagcaagggcgaggaggataacatgg	Amplify mCherry F
BBC206	tgtaggctggagctgcttcttacttgtacagctcgtccatg	Amplify mCherry R
ABD255	gaagcagctccagcctacaCCACAATAAGCCAGAGAGCCTTAAG	Insert construct at *lacZ* F2
ABD256	CCCAAATACGGCAACTTGGCG	Insert construct at *lacZ* R2
Primers for TfoS Constructs		
Primer	**Sequence**	**Description**
ABD332	GGCTGAACGTGGTTGTCGAAAATGAC	Insert construct at *lacZ* F1
BBC244	CCCGGGATCCTGTGTGAAATTGTTATCCGC	Insert construct at *lacZ* Zeo^{R} R1
BBC4343	caatttcacacaggatcccgggAGGAGGTGAACTCaTGTTTCGCACATTG	Amplify TfoS for Ptac F
BBC2476	tgtaggctggagctgcttcTTAGTTTTCTTGATCTTCGATGAATTGGC	Amplify TfoS for Ptac R
ABD255	gaagcagctccagcctacaCCACAATAAGCCAGAGAGCCTTAAG	Insert construct at *lacZ* F2
ABD256	CCCAAATACGGCAACTTGGCG	Insert construct at *lacZ* R2
ABD640	GCAATACACGCTGTGTTTCACCG	Amplify native TfoS F1
CKP760	tccaccacttccacctgcATTTCTCACTTCAAGTTGTATGG	Insert tag after TfoS N929 R1
BBC2274	gcaggtggaagtggtggagattataaggatgacgatgacaaagcaggtggagcaggtgga	1X FLAG F
BBC2275	tccacctgctccacctgctttgtcatcgtcatccttataatctccaccacttccacctgc	1X FLAG R
CKP761	gcaggtggagcaggtggaGCGCAGGCGGTTATCGTATTTTC	Insert tag after TfoS N929 F2
ABD643	TCGTTTTCTAAGGCTCGAATCGCC	Amplify native TfoS R2
Primers for TfoR Constructs		
Primer	**Sequence**	**Description**
BBC4983	GTGATACCACAAGCAACTATACC	TfoR F1
BBC4980	gcttaatcatgtttttaaggtgttgattttaACCTAAGCAAACATTGTTTTCG	Delete CBS in PtfoR R1
BBC4981	cgaaaacaatgtttgcttaggtTAAAATCAACACCTTAAAAACATGATTAAGC	Delete CBS in PtfoR F2
BBC4984	TCGTGCAACTTGAGAGTAACAAC	TfoR R2
VGP0478	tagaataggtactaatcagaatagtgaggagACCTAAGCAAACATTGTTTTCG	Insert 4X tetO in PtfoR R1
VGP0480	CTCCTCACTATTcTGATTAGTACC	Amplify 4X tetO F
BBC4338	CTCATTAGGCACtCCAGGC	Amplify 4X tetO R
VGP0479	gcctggagtgcctaatgagTAAAATCAACACCTTAAAAACATGATTAAGC	Insert 4X tetO in PtfoR F2
BBC706	CCACACATTATACGAGCCGATG	Amplify TfoR for Ptac R1
BBC708	CATCGGCTCGTATAATGTGTGGATTCCAGAGGTGGTATGACC	Amplify TfoR for Ptac F2

774